

Article

Optimal Planning of Solar Photovoltaic (PV) and Wind-Based DGs for Achieving Techno-Economic Objectives across Various Load Models

Habib Ur Rehman ¹, Arif Hussain ², Waseem Haider ^{2,*}, Sayyed Ahmad Ali ¹, Syed Ali Abbas Kazmi ^{1,*}
and Muhammad Huzaifa ¹

- ¹ US-Pakistan Center for Advanced Studies in Energy (USPCAS-E), National University of Sciences and Technology (NUST), H-12, Islamabad 44000, Pakistan
² Department of Electrical and Computer Engineering, Sungkyunkwan University, Seoul 16419, Republic of Korea
* Correspondence: haider@skku.edu (W.H.); saakazmi@uspcase.nust.edu.pk (S.A.A.K.)

Abstract: Over the last few decades, distributed generation (DG) has become the most viable option in distribution systems (DSs) to mitigate the power losses caused by the substantial increase in electricity demand and to improve the voltage profile by enhancing power system reliability. In this study, two metaheuristic algorithms, artificial gorilla troops optimization (GTO) and Tasmanian devil optimization (TDO), are presented to examine the utilization of DGs, as well as the optimal placement and sizing in DSs, with a special emphasis on maximizing the voltage stability index and minimizing the total operating cost index and active power loss, along with the minimizing of voltage deviation. The robustness of the algorithms is examined on the IEEE 33-bus and IEEE 69-bus radial distribution networks (RDNs) for PV- and wind-based DGs. The obtained results are compared with the existing literature to validate the effectiveness of the algorithms. The reduction in active power loss is 93.15% and 96.87% of the initial value for the 33-bus and 69-bus RDNs, respectively, while the other parameters, i.e., operating cost index, voltage deviation, and voltage stability index, are also improved. This validates the efficiency of the algorithms. The proposed study is also carried out by considering different voltage-dependent load models, including industrial, residential, and commercial types.

Keywords: artificial gorilla troops optimization; distributed generation; distributed system; operating cost; radial distribution network; Tasmanian devil optimization; voltage deviation; voltage stability index



Citation: Rehman, H.U.; Hussain, A.; Haider, W.; Ali, S.A.; Kazmi, S.A.A.; Huzaifa, M. Optimal Planning of Solar Photovoltaic (PV) and Wind-Based DGs for Achieving Techno-Economic Objectives across Various Load Models. *Energies* **2023**, *16*, 2444. <https://doi.org/10.3390/en16052444>

Academic Editor: Mohd. Hasan Ali

Received: 4 January 2023
Revised: 20 February 2023
Accepted: 24 February 2023
Published: 3 March 2023



Copyright: © 2023 by the authors. Licensee MDPI, Basel, Switzerland. This article is an open access article distributed under the terms and conditions of the Creative Commons Attribution (CC BY) license (<https://creativecommons.org/licenses/by/4.0/>).

1. Introduction

Due to a rapidly increasing population, the consumption of electricity has likewise increased. As a result, the performance of distribution systems (DSs) has been decreased because of greater power losses and voltage drops due to the higher R/X ratio in the existing DSs [1]. To meet the rising demand for electricity, electric utility companies are constantly planning to expand their existing electrical systems. The conventional planning approach is to build a new grid or enlarge an existing one [2]. However, this is not a feasible solution in economic and environmental terms, as most of the existing networks are radial in nature and are powered by fossil fuels [3], which affects the environment through the emission of harmful gases. Thus, an attractive substitution to meet this rising demand is the use of distributed generation (DG) in DSs. DGs such as PV and wind are small power sources installed near to the end users [4]. Due to the environmentally friendly, reliable, and cost-effective benefits of renewable DGs such as solar and wind power, etc., these power sources are now extensively used to generate energy on a larger scale [5,6]. DGs play a vital role in enhancing the DSs' efficiency and reliability by decreasing power losses and

voltage drops and enhancing voltage stability. However, the improper allocation of DGs has an adverse effect on the DSs' performance by increasing the power losses and voltage drops and reducing the voltage stability of the network. Thus, to enhance the system's technical, economic, and environmental benefits, the optimal allocation of DGs (OADG) in DSs needs to be established cautiously.

The optimal placement and sizing of DGs in DS present a challenging problem in the literature. Therefore, researchers have taken various studies and developed different optimization methods, including analytical and metaheuristic approaches, to address the problem of OADG with different operating requirements for optimizing a single-objective function (SOF) and multi-objective function (MOF). In Ref. [7], a simplified analytical technique has been suggested for determining OADG and the optimal power factor (OPF) to enhance the active power loss (APL) reduction for three different radial distribution systems (RDSs), i.e., IEEE 12-, 33-, and 69-bus RDSs. To enhance the APL reduction, voltage profile, and economic benefits, an analytical approach has been recommended in Ref. [8] for determining the optimal placement and sizing of various types of DGs. The effectiveness of the suggested approach was also validated by testing on standard IEEE 33- and 69-bus RDSs for different loading scenarios. A modified version of the analytical method has been developed by the authors of [9] for OAPVDG, with the aim of enhancing the economic benefits and technical benefits (APL reduction and voltage stability margin enhancement) offered by DS planning. For defining the optimal placement of DGs, the line loss sensitivity factor (LSF) was utilized, while particle swarm optimization (PSO) with a constriction factor was employed for ascertaining the optimal DG capacity. The described approach was examined on IEEE 33-bus RDS. The authors of [10] proposed a MINLP model, solved through GAMS, for determining the OADG, with the aim of improving PL reduction. To validate the robustness of the approach, two standard test systems, IEEE 33- and 69-bus RDSs, were used. The proposed approach was also employed on a real 27-node test DS to optimally locate a PV-DG, assuming a sunny day. In another study [11], a new VSI-based LQP index was utilized to find the optimal DG location, while optimal DG capacity was ascertained by reducing APL. The suggested approach was examined on an IEEE 33-bus RDS. In Ref. [12], the voltage stability margin index (VSMI) was utilized to find the optimal placement of DG; optimal DG capacity was ascertained using the curve-fitting technique (CFT). The suggested approach was examined on IEEE 33- and 69-bus RDSs. In Ref. [13], a decision-making algorithm has been developed for ascertaining the OADG of different types with the aim of minimizing total APL and QPL and improving the voltage profile of the DSs. The suggested method was tested on an IEEE 33-bus RDS. A heuristic approach has been suggested in one study [14] for determining OADG and capacitor banks (CBs) to minimize the APL and enhance the voltage profile of the DSs. The described technique was tested on IEEE 33-, 69- and 119- test bus RDSs at OPF.

Analytical approaches are used wherein the DGs are placed one by one; however, these are not suitable for a multi-objective problem as their accuracy is incompatible with the integration of multiple DGs. The solution obtained by MILP is least consistent for complex problems due to the linearization nature of the algorithm, while heuristic algorithms offer a feasible solution with greater accuracy compared to linearized approaches with a higher computational burden. Metaheuristic methods are used globally, due to their easy implementation, to solve multi-objective problems with robust searching capabilities. Although metaheuristic algorithms do not ensure optimality, they offer feasible and efficient solutions with improvements in accuracy to converge the solution, compared to MILP and the heuristic approach to solving complex problems.

Due to their robust searching abilities to calculate the optimal solution for larger DNs, metaheuristic techniques have been widely used to solve the problem of OADG in DSs with SOFs and MOFs. In SOFs, only a single objective is optimized, while optimizing multiple objectives simultaneously is considered more suited to MOFs. Most of the metaheuristic techniques, such as multileader particle swarm optimization (MLPSO) [1], the improved stochastic fractal search algorithm (CFSA) [15], fine-tuned PSO [16], the strawberry plant

propagation algorithm (SPPA) [17], and Aquila optimization (AO) [18], used SOF to allocate multiple DGs for minimizing the APL while enhancing the voltage profile of the system. Moreover, to minimize the APL and enhance the voltage profile, a hybrid of binary PSO and shuffled frog leap (SLFA), BPSO-SLFA, has been proposed by the authors of [19] for solving the OADG problem, along with network configuration. The suggested algorithm was tested on standard IEEE 33- and 69-bus RDSs. An improved version of forensic-based investigation (FBI), quasi oppositional FBI (QOBI) has been recommended by the authors of [20] for solving the problem of optimal placement and sizing, along with the OPF of various types of DGs, with the aim of minimizing the APL and improving the voltage profile of the system. In Ref. [21], the authors proposed the Coulomb–Franklin algorithm (CFA) for OADG, along with capacitor banks (CBS) in DS, to minimize the APL. The above-mentioned techniques were only implemented for a constant power load model. The authors of [22] suggested using a genetic algorithm (GA) for solving the problem of OADG, to minimize the APL while enhancing the voltage profile of the system. The suggested algorithm was validated on a standard IEEE 33-bus RDS with different load states and load models by considering the daily and yearly load profiles.

Compared with SOFs, MOFs are used to optimize multiple objectives simultaneously by converting them into SOFs through various multi-objectivity methods. To optimize the MOF based on the reduction of APL, VD, and VSI maximization for solving the problem of optimal placement and the sizing of multiple and various types of DGs in DN, different multi-objectivity methods have been employed using various metaheuristic techniques. A quasi-oppositional chaotic symbiotic organism search (QOCSOS) [23], quasi-oppositional differential evolution Lévy flights algorithm (QODELFA) [24], manta ray foraging optimization (MRFO) [25], and improved grey wolf optimizer-PSO (I-GWOPSO) [26] have used the weighted sum method, while an improved decomposition-based evolutionary algorithm (I-DBEA) [27] used the e-constraints method; the chaotic sine cosine algorithm (CSCA) [28], and an improved Harris hawk optimization (IHHO) method [29] used grey relation analysis to find the best optimal solution from a Pareto optimal solution. An enhanced artificial ecosystem-based optimization (EAEO) algorithm [30] used a fuzzy decision-making approach to find the best optimal solution from the Pareto optimal solution, while adaptive PSO and gravitational search algorithm (GSA) approaches have used the Pareto optimal front, e-constraints, and aggregated sum methods. Moreover, to solve MOFs based on technical (APL, VD, and VSI), economic (cost of CB and the cost of power produced), and environmental (pollutant emissions) objective improvements for aiming the OADG and CB, the salp swarm algorithm (SSA) [31] was used with the weighted sum method. A multi-objective differential evolution (MODE) algorithm [32] has used a fuzzy approach to solve the MOF for improving technical, economic, and environmental objectives. The suggested approach was implemented on standard IEEE 33-, 69-bus, and 62-bus real RDSs. In another study [33], the authors introduced a multi-objective firefly algorithm (MOFA) to minimize the PL, VD, THD, the cost of DG, and GHG emissions and maximized the VSI as a MOOP for ascertaining the optimal allocation of DG (OADG) The optimal solution was determined using a fuzzy decision-making approach. The recommended system was tested on an IEEE 33-bus RDN and an actual 62-bus Indian distribution system.

In Ref. [34], the hybrid optimization technique (GSA + GAMS) was implemented for OADGs (solar, wind, and hydropower sources) with network reconfiguration in DN to optimize the MOF, based on the improvement of technical (APL) and economic (cost) benefits. In this study, the authors used GSA to find the optimal placement of DGs and the optimal capacity of DG GAMS. To check the validity and effectiveness of the algorithm, a standard IEEE 33-bus RDN and a real-time varying DN were utilized. A multi-objective opposition-based chaotic differential evolution (MOCDE) algorithm has been proposed by the authors of [35] to solve the OADG problem for optimizing the MOF to achieve technical objectives (minimization of PL and reduction of VD); and economic objective (minimization of yearly economic loss cost). The suggested algorithm was tested on standard IEEE 33- and 69-bus RDNs. In Ref. [36], the author introduced the artificial bee colony (ABC)

optimization algorithm for the optimal siting and sizing of DGs to minimize the APL, voltage drops, and total energy costs concurrently, as a multi-objective problem (MOP). The suggested algorithm was tested on standard IEEE 33- and 69-test-bus RDNs.

An opposition-based chaotic differential evolution (OTCDE) system was proposed in Ref. [37] for OADG, to deal with MOPs consisting of technical (voltage deviation and line flow capacity) and economic objectives. The proposed system was tested on standard IEEE 33-, 69-, and 118-bus RDNs. The stud krill herd algorithm (SKHA) [38] was recommended to solve the problem of OADG in DN for optimizing MOFs, based on APL, VD, and OC. The MOF in question was solved using the weighted sum approach. In Ref. [39], the authors proposed an ant colony optimization (ACO) algorithm for the optimal allocation of renewable-based DGs with the aim of optimizing MOFs, based on the APL index, VD index, and OCI. The suggested approach was tested on an IEEE 33-bus and actual 85-bus Indian DS. The authors of [40] proposed an artificial hummingbird algorithm (AHA) to solve the problem of the optimal allocation of renewable DGs considering uncertainties for optimizing the MOF, based on APL, VD, VSM, and total annual energy savings, using the weighted sum method. The suggested technique was tested on a standard IEEE 33- and 69-bus RDS for different load states. A comprehensive review of the optimization methods used for OADG to achieve different objectives is presented in Table 1.

Table 1. Summary of optimization techniques used for OADG in RDNs.

Ref.	Year	Optimization Methods	Objective Functions					Load Model
			APL	QPL	VD	VSI	Cost	VP
[7]	2019	Analytical	✓	✗	✗	✗	✗	✗
[41]	2019	ASFL	✓	✗	✗	✓	✗	✗
[42]	2019	BBO	✓	✗	✗	✗	✗	✗
[43]	2019	MOHTLGOGWO	✓	✗	✗	✗	✗	✗
[15]	2019	CSFS	✓	✗	✗	✗	✗	✗
[44]	2019	LSF + GWO	✓	✗	✗	✓	✗	✗
[22]	2019	GA	✓	✗	✗	✗	✗	✓
[12]	2019	VSMI + CFT	✓	✗	✗	✗	✗	✗
[14]	2019	Heuristic	✓	✗	✗	✗	✗	✗
[24]	2019	QODELFA	✓	✗	✓	✓	✗	✗
[1]	2020	MLPSO	✓	✗	✗	✗	✗	✗
[23]	2020	QOCSOS	✓	✗	✓	✓	✗	✗
[45]	2020	IRRO	✓	✓	✓	✓	✓	✗
[28]	2020	CSCA	✓	✗	✓	✓	✗	✗
[37]	2020	OTCDE	✓	✗	✓	✗	✓	✗
[30]	2020	EAE0	✓	✗	✓	✓	✗	✗
[46]	2020	APSO and MGSA	✓	✗	✓	✓	✗	✗
[10]	2020	MINLP(GAMS)	✓	✗	✗	✗	✗	✗
[29]	2020	IHHO	✓	✗	✓	✓	✗	✗
[47]	2020	PSO and MOPSO	✓	✗	✓	✗	✗	✗
[19]	2020	BPSO-SLFA	✓	✗	✗	✗	✗	✗
[48]	2020	MSMO	✗	✗	✓	✗	✗	✗
[25]	2020	MRFO	✓	✗	✓	✓	✗	✗

Table 1. Cont.

Ref.	Year	Optimization Methods	Objective Functions					Load Model	
			APL	QPL	VD	VSI	Cost	VP	
[49]	2020	PPA	✓	✗	✗	✗	✗	✗	
[27]	2021	I-DBEA	✓	✗	✓	✓	✗	✗	
[36]	2021	ABC	✓	✗	✓	✗	✓	✗	
[50]	2021	BAT	✓	✗	✗	✓	✗	✓	
[16]	2021	Fine tuned PSO	✓	✗	✗	✗	✗	✗	
[17]	2021	SPPA	✓	✗	✗	✗	✗	✗	
[38]	2021	SKHA	✓	✗	✓	✗	✓	✗	
[8]	2022	Analytical	✓	✗	✗	✗	✗	✗	
[51]	2022	Improve MOPSO	✓	✗	✗	✓	✗	✗	
[33]	2022	POFA	✓	✗	✓	✓	✓	✗	
[26]	2022	I-GWOPSO	✓	✗	✓	✓	✗	✗	
[39]	2022	ACO	✓	✗	✓	✗	✓	✗	
[21]	2022	CFA	✓	✗	✗	✗	✗	✗	
[20]	2022	QOFBI	✓	✗	✗	✗	✗	✗	
[18]	2022	AO	✓	✗	✗	✗	✗	✗	
[52]	2022	Modified FPA	✓	✗	✗	✗	✗	✓	
[53]	2023	Mixed integer GA	✓	✗	✓	✗	✗	✗	
[54]	2023	MOWOA	✓	✗	✗	✗	✓	✗	
[55]	2023	NSGA-II	✓	✗	✓	✗	✓	✗	
[P]	2023	TDO, GTO	✓	✓	✓	✓	✓	✓	

Note: P—Proposed; VP—voltage-dependent (variable) power.

It can be seen from Table 1 that various optimization methods had been investigated for solving the problem of the optimal allocation of DGs for achieving technical and economic objectives while considering only the constant power (CP) load model by optimizing SOF and MOF. Very few studies have considered VP load models. However, in some [50,52], voltage-dependent load models have been utilized to solve the problem of OADG, to achieve only technical objectives. In this study, two metaheuristic algorithms, Tasmanian devil optimization (TDO) and artificial gorilla troops optimization (GTO), are proposed. The application of TDO and GTO algorithms is employed in the field of engineering to solve complex problems. The reason for using these metaheuristic algorithms is that their ability to solve complex and high-dimensional problems is more efficient than other metaheuristic algorithms, such as PSO and GA, due to their ability to explore and exploit phases efficiently. Every metaheuristic algorithm has its pros and cons. In terms of solving high-dimensional and complex problems, GTO and TDO perform well in finding a globally optimal solution by balancing between exploration and exploitation phases, while GA and PSO trap into local minima and demand high computational time. The tuning of the parameters in PSO is also the main issue that led to premature convergence. The main issue of the GTO algorithm is its longer running time. Although the run-time of the GTO algorithm is longer, it is, however, useful as it is capable of solving high-dimensional problems with higher performance. To check the performance of the TDO and GTO algorithms, they are compared with other well-known optimization algorithms that validate the effectiveness of the algorithms for solving the problem of the optimal allocation of DGs.

Thus, in this study, the CP load model, as well as VP load models, are considered to solve the problem of OADG in DN, to achieve techno-economic objectives by optimizing SOF and MOF. The following are the main contributions of this paper:

- The proposed optimization algorithms are identified as GTO and TDO.
- The proposed techniques are analyzed for renewable DGs such as Photovoltaic (PV) type and wind turbine (WT) type at unity and combined power factor (pf).
- The GTO and TDO techniques address the OADG problem to minimize APL and QPL using SOF.
- The GTO and TDO techniques address the OADG problem to improve APL reduction, VD, VSI, and OCI (the investment, operation, and maintenance costs of DG) concurrently with the MOF.
- The robustness of the proposed algorithms is examined on two standard test bus systems, i.e., IEEE 33- and 69-bus RDNs, and are compared with each other.
- The proposed techniques are further explored for voltage-dependent load models consisting of residential, commercial, and industrial load models, which make the problem more practical than with the CP load model.
- The proposed techniques generate a better result than the existing optimization techniques, which validates the methodology.
- The proposed GTO technique outperforms the other proposed TDO techniques in terms of convergence characteristics and optimizing the SOF.

The remainder of this paper is organized as follows: Section 2 represents the problem formulation, including the objective functions, with system constraints and load modeling. Section 3 introduces the summary of proposed algorithms, i.e., TDO and GTO. In Section 4, the simulation results and discussions are presented. Finally, the conclusions are presented in Section 5.

2. Problem Formulations

The main objective of this study is to optimally allocate the DGs to solve the SOF and MOF. The SOF includes the reduction of total power losses, i.e., APL and QPL, while the MOF includes the reduction of APL, minimization of VD, maximization of VSI, and minimization of total OC, including investment, operation, and the maintenance costs of DGs.

2.1. Objective Functions

The mathematical modeling for SOF and MOF is presented in the following subsections.

2.1.1. Reduction of Active Power Loss (APL)

In the RDN, the APL is computed using the following equation [26,56]:

$$APL = \sum_{j=1}^{M_{br}} |I_j|^2 \cdot R_j \quad (1)$$

Here, j is a branch number, the total number of branches is represented by M_{br} , and $|I_j|$ represents the absolute current passing through the branch of resistance, R_j . The first objective function (OF_1) is represented as:

$$OF_1 = \text{Min}(APL) . \quad (2)$$

2.1.2. Reduction of Reactive Power Loss (QPL)

In the RDN, the QPL is computed using the following equation:

$$QPL = \sum_{j=1}^{M_{br}} |I_j|^2 \cdot X_j . \quad (3)$$

Here, j is a branch number, the total number of branches is represented by M_{br} , and the absolute current $|I_j|$ represents the absolute current passing through the branch of inductive reactance, X_j . The second objective function, OF_2 , is represented as:

$$OF_2 = \text{Min} (QPL) . \tag{4}$$

2.1.3. Minimization of Voltage Deviation (VD)

The lifetime and performance of the equipment are affected by the deviation of the voltages. Therefore, we keep in mind that the reason for the minimization of voltage deviation is taken as OF. VD is calculated using the following equation [57]:

$$VD = \sum_{j=1}^m (V_{ref} - V_j)^2 \tag{5}$$

where V_{ref} denotes the reference voltage of value, 1.0 p.u. The “ m ” denotes the number of total buses in the radial distribution system, whereas “ V_j ” denotes the voltage of the receiving bus. The third OF (OF_3) is represented as:

$$OF_3 = \text{Min} (VD) . \tag{6}$$

2.1.4. Minimization of Voltage Deviation (VD)

Along with VD, VSI is another crucial component to take into account when determining the security level of the DN. Due to a variety of factors, when a bus in a DN exceeds the permitted voltage limits, the entire system may experience voltage instability, or VSI. All the buses in a DN must maintain VSI at a stable limit for steady operation. Equation (7) is used to compute the VSI [41]:

$$VSI_{(k+1)} = |V_k|^4 - 4 \left(P_{(k+1)}x_k - Q_{(k+1)}r_k \right)^2 - 4 |V_k|^2 \left(P_{(k+1)}r_k - Q_{(k+1)}x_k \right) . \tag{7}$$

In Equation (7), $P_{(k+1)}$ and $Q_{(k+1)}$ represent the real and reactive load demands, respectively; the k represents the sending bus number, and V_k denotes the voltage of the sending bus, whereas the line resistance is denoted by r_k and the line reactance is represented by x_k , which feed the receiving bus ($k + 1$). For the secure and stable operation of the RDN, the VSI value must be greater than zero. The fourth OF (OF_4) is represented as:

$$OF_4 = \text{Max} \left(\text{Min} \left(VSI_{(k+1)} \right) \right) . \tag{8}$$

2.1.5. Minimization of Operating Cost Index (OCI)

The total price for obtaining electricity from the grid consists of the power loss price and the price of the power supplied to the customer. The total operating cost before DG integration is computed using the following equation [39]:

$$OC_{base} = \sum_{t=1}^{Tp} PWF^t \times (P_L + P_{Tload}) \times T \times C_e \tag{9}$$

where P_L denotes the power loss in the base case and P_{Tload} denotes the supplying power to the customer, while T refers to the time period (hr/year), Tp refers to the planning years and the cost of energy, and price, C_e , is 49 (USD/MWh). PWF is a present worth factor and is evaluated as:

$$PWF = \frac{1 + \text{inf}_R}{1 + \text{int}_R} \tag{10}$$

Here, inf_R is the inflation rate, with a value of 9%, and int_R is the interest rate, with a value of 12.5%.

The annual operational cost can be broken down into the following four elements. The first element is the maintenance cost of DG, which is determined using the following equation:

$$DG_m = \left(\sum_{t=1}^{Tp} \sum_{i=1}^{Ndg} PWF^t \times P_{DG,i} \times T \times K_{M, DG} \right) \quad (11)$$

where $K_{M, DG}$ denotes the DG maintenance cost and its value is taken as 7 (USD/MWh), $P_{DG,i}$ represents the power of installed DG, and Ndg represents the number of DG installed units.

The second element is the DG operational cost, which is computed through the following equation:

$$DG_O = \left(\sum_{t=1}^{Tp} \sum_{i=1}^{Ndg} PWF^t \times P_{DG,i} \times T \times K_{O, DG} \right) \quad (12)$$

where $K_{O, DG}$ denotes the DG operation cost and its value is taken as 29 (USD/MWh).

The third component is the DG installation cost, which is computed through the following equation:

$$DG_{IC} = K_{IC, DG} \sum_{i=1}^{Ndg} P_{DG, i} \quad (13)$$

where $K_{IC, DG}$ is the DG installation cost and its value is taken 400,000 (USD/MWh).

The last element is the cost of operation after DG integration, which is calculated using the following equation:

$$OC_{DG} = \sum_{t=1}^{Tp} PWF^t \times (P_L + P_{Tload}) \times T \times C_e \quad (14)$$

where P_L denotes the power loss after integrating DG and P_{Tload} denotes the supplying power to the customer.

Thus, the annual operating cost can be constructed as:

$$OC_{TDG} = DG_M + DG_O + DG_{IC} + OC_{DG}. \quad (15)$$

The fifth OF (OF_5) is represented as:

$$OF_5 = \text{Min} \left(\frac{OC_{TDG}}{OC_{base}} \right). \quad (16)$$

2.2. Formulation of a Multi-Objective Function (MOF)

Unlike SOFs, in MOFs, two or more conflicting objective functions are dealt with simultaneously. To establish the TEOF, each of the objective functions is divided by its base value and corresponding weight. For MOFs, the weighted sum method is used. The TEOF is formulated as:

$$TEOF = \text{Min} \left(\alpha_1 \times \frac{RPL}{RPL_{base}} + \alpha_2 \times \frac{TVD}{TVD_{base}} + \alpha_3 \times \frac{VSI^{-1}}{VSI_{base}^{-1}} + \alpha_4 \times \frac{OC_{TDG}}{OC_{base}} \right), \quad (17)$$

and

$$\sum_{i=1}^4 \alpha_i = 1; \alpha \in [0, 1], \quad (18)$$

where RPL_{base} , TVD_{base} , VSI_{base}^{-1} and OC_{base} are the base values of real power losses, total voltage deviation, the voltage stability index and operating cost, respectively. α_1 , α_2 , α_3 , and α_4 are the different weights given to the individual objective function. Their values

are 0.5, 0.35, 0.15, and 0.1, respectively. The preference for weights shown is given to the technical objectives over the economic objective.

2.3. System Constraints

The MOF that is calculated in Equation (17) is subjected to the following constraints.

2.3.1. Equality Constraints

The flow of powers in the distribution system must be balanced. In other words, the power drawn from the substation and the power generated from the DG units should be sufficient to meet the following requirements for load demand and power losses [39]:

$$P_s + \sum_{i=1}^{Ndg} P_G(i) = P_D + APL \quad (19)$$

$$Q_s + \sum_{i=1}^{Ndg} Q_G(i) = Q_D + QPL \quad (20)$$

where P_s and Q_s are the active and reactive powers drawn from the substation, respectively. P_G and Q_G are the incoming powers that are generated from the installed DG units. P_D , Q_D , RPL , and QPL are the active and reactive load demands and the real and reactive power losses, respectively.

2.3.2. Inequality Constraints

Voltage Limits

The voltage magnitude of the bus in the network should be within permissible limits; that is, they can be expressed as [26,58]:

$$0.95 \text{ p.u.} \leq V_i \leq 1.05 \text{ p.u.} \quad (21)$$

Branch Current Limits

The maximum limit of a branch's current should not be exceeded [26], as stated by:

$$I_{j,i} \leq I_{j,i}^{max}. \quad (22)$$

DG Capacity Limits

The range of the output power of DG units is expressed as [39,43]:

$$P_G^{min} \leq P_G \leq P_G^{max} \quad (23)$$

$$Q_G^{min} \leq Q_G \leq Q_G^{max}. \quad (24)$$

DG power factor limit

The following range of power factors can be used to operate DG units [26,44]:

$$p \cdot f_{DG}^{min} \leq p \cdot f_{DG} \leq p \cdot f_{DG}^{max}. \quad (25)$$

2.4. Load Modeling

Most of the studies in the literature have focused on the power flow issue using constant load models, or constant active and reactive powers. However, actual load characteristics show how much load power depends on the bus voltage. The distribution system's load can often be divided into three categories: industrial, residential, and commercial loads. In this study, a real-life problem is considered by modeling voltage-dependent load

industrial, residential, and commercial load models. The mathematical formulation of voltage-dependent load models is expressed as:

$$P = P_o V_n^\alpha \quad (26)$$

$$Q = Q_o V_n^\beta \quad (27)$$

where active and reactive powers are represented by P and Q , respectively; P_o and Q_o refer to the values of active and reactive powers at nominal voltage, respectively; V_n denotes the magnitude of the voltage, whereas α and β are the values of the active and reactive power exponents. The values of the α and β used in this study for various types of loads are shown in Table 2, which has been taken from Refs. [50,58].

Table 2. Load types and exponent values.

Load Types	α	β
Constant	0	0
Residential	0.92	4.04
Commercial	1.51	3.40
Industrial	0.18	6.0

3. Methodology

The aim of this study is to use a metaheuristic algorithm to optimize the SOF and MOF, based on APL, VD, VSI, and OCI for the optimal allocation of DGs in DN. In this section, two newly metaheuristic optimization algorithms, named artificial gorilla troops optimization (GTO) and Tasmanian devil optimization (TDO), are presented.

3.1. Artificial Gorilla Troop Optimization (GTO)

In 2021, Abdollahzadeh and Miralilli [59] introduced a novel bio-inspired metaheuristic algorithm, named gorilla troop optimization (GTO), based on gorilla group behavior in the wild when finding food and living as a troop. Each troop has a silverback gorilla that serves as the troop's leader; it is responsible for ensuring the safety of the troop by taking crucial decisions. The silverback gorilla is supported by young male gorillas (known as black-backs) to provide backup protection for the group.

As with other optimization techniques, for optimization operation, two phases are used by the GTO algorithm, known as the exploration and exploitation phases.

3.1.1. Exploration Phase

In GTO, three different strategies are used for the exploration phase. In the first strategy, the gorilla moves toward an unknown place, while in the second strategy, the gorilla moves in the direction of another gorilla; in the third strategy, it moves to a known place. The X and GX represent the position of the gorilla and the silverback, respectively. The following are expressions for the mathematical formulas used in this phase:

$$GX(t+1) = (ub - lb) * R1 + lb, \text{ rand} < P \quad (28a)$$

$$GX(t+1) = (R2 - C) * Xr(t) + L * H, \text{ rand} \geq 0.5 \quad (28b)$$

$$GX(t+1) = X(i) - L * (L * (X(t) - GXr(t)) + R3 * (X(t) - GXr(t))), \text{ rand} < 0.5. \quad (28c)$$

In Equation (28), ub and lb represent the upper and lower bound, respectively. $R1$, $R2$, and $R3$ are random numbers in the range of $[0, 1]$, whereas t represents the current iteration. p is a predetermined value in the interval of $[0, 1]$, which is used to select the movement of the gorilla to an unknown site, as in the above strategies. $rand$ denotes the random value in

the interval of 0-1. GX_r and X_r are the randomly selected solutions from the population, whereas other parameters are calculated using Equations (29), (31) and (32):

$$C = F * \left(1 - \frac{it}{maxit}\right) \quad (29)$$

$$F = \cos(2 * R4) + 1 \quad (30)$$

$$L = C * l \quad (31)$$

$$H = Z * X(t) \quad (32)$$

$$Z = [-C, C] \quad (33)$$

where it and $maxit$ denote the current and max number of iterations, respectively. $R4$ is a random parameter in the range of 0–1. The value of l is in the range of $[-1, 1]$.

3.1.2. Exploitation Phase

In the exploitation phase, two different mechanisms are used; either the gorilla's troop follows the silverback gorilla's decision or it competes for the adult females. The probability of selecting the mechanism is based on the value of C . If $C \geq W$, the gorilla's troop follows the silverback's instructions. This behavior is shown as follows:

$$GX(t + 1) = L * M * (X(t) - X_{silverback}) + X(t) \quad (34)$$

$$M = \left(\left| \frac{1}{N} \sum_{i=1}^N GX_i(t) \right|^g \right)^{\frac{1}{g}} \quad (35)$$

$$g = 2^L \quad (36)$$

where the silverback's position is represented by $X_{silverback}$. If $C < W$, competition for the adult females is selected and this behavior is expressed as follows:

$$GX(i) = X_{silverback} - (X_{silverback} * Q - X(t) * Q) * A \quad (37)$$

$$Q = 2 * R5 - 1 \quad (38)$$

$$A = \beta * E \quad (39)$$

$$E = \begin{cases} N_1, & rand \geq 0.5 \\ N_2, & rand < 0.5 \end{cases} \quad (40)$$

where Q represents impact force, $R5$ is a random number in the interval $[0, 1]$, and β is a predefined variable. The value of $rand$ is between 0 and 1. "E" will be equal to random values in the problem matrix and the Gaussian distribution, when $rand \geq 0.5$; conversely, "E" will be from just the Gaussian distribution, when $rand < 0.5$. A flow chart showing the process of the GTO technique to address OADG in DN is depicted in Figure 1 and an explanation of the flow chart is described in Algorithm A1 in the Appendix A section.

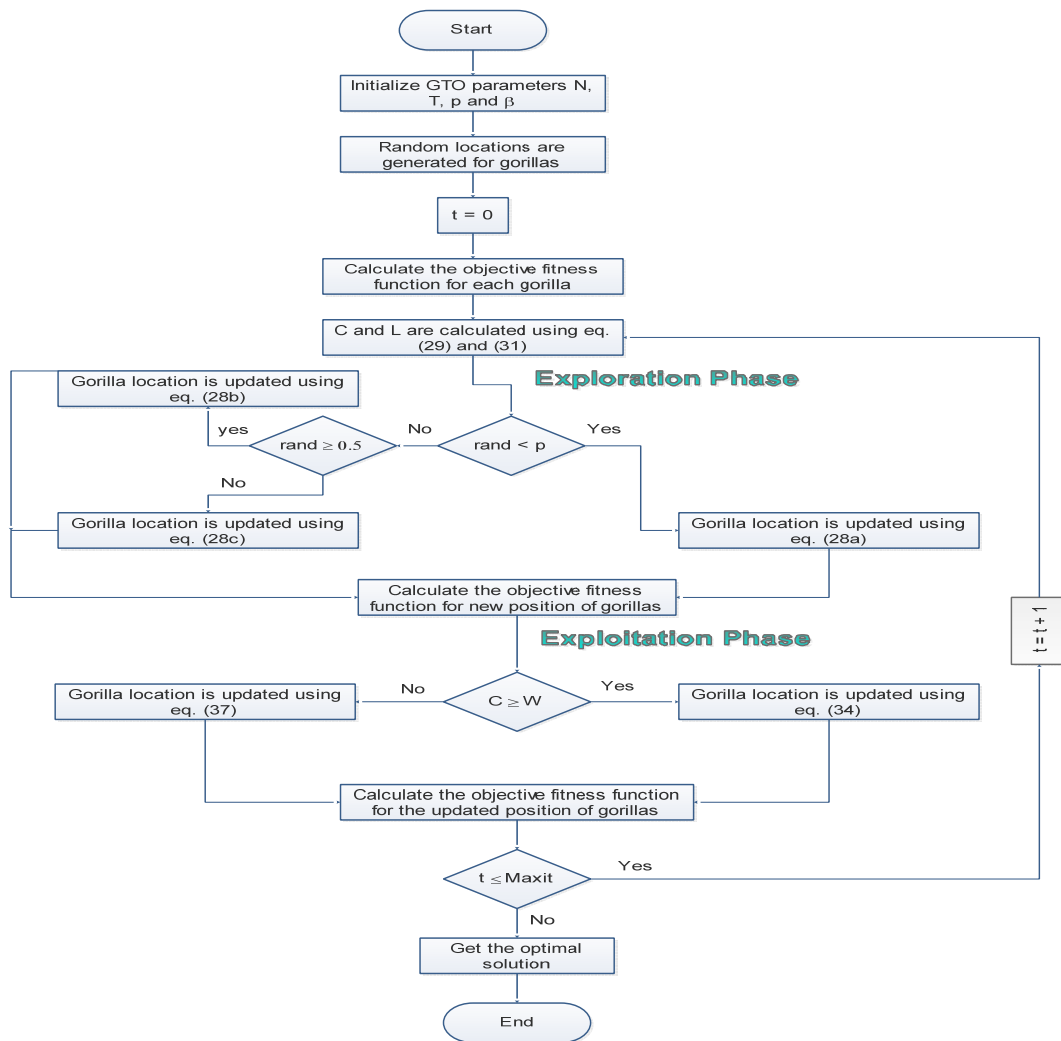


Figure 1. Flow chart of the GTO algorithm to solve the problem of OADG.

3.2. Tasmanian Devil Optimization (TDO)

In 2022, Dehghani introduced a novel bio-inspired metaheuristic algorithm [60], named the Tasmanian devil optimizer (TDO), based on the Tasmanian devil's behavior in the wild during feeding. Two different approaches/strategies are used by the Tasmanian devil during the feeding process. The first one is eating carrion, while the second is eating prey. The mechanism of these approaches is discussed below.

3.2.1. Feeding by Eating Carrion (Exploration Phase)

In the TDO algorithm, the Tasmanian devil's approach to feeding by eating carrion is mathematically designed using Equations (41) and (42). The process of choosing carrion is mimicked in Equation (41):

$$C_i = X_k, \quad i = 1, 2, 3, \dots, N, \quad k \in \{1, 2, \dots, N | k \neq i\} \quad (41)$$

where C_i denotes the carrion selected by the i th Tasmanian devil and X represents the Tasmanian devil population. A new position for the Tasmanian devil within the search space is determined, based on the chosen carrion. The updated location of the Tasmanian devil can be formulated using Equation (42).

$$x_{i,j}^{new, S1} = \begin{cases} x_{i,j} + r * (c_{i,j} - l * x_{i,j}), & F_{C_i} < F_i \\ x_{i,j} + r * (x_{i,j} - c_{i,j}), & otherwise \end{cases} \quad (42)$$

In Equation (42), $x_{i,j}$ represents the candidate value from the candidate solution for the j th variables, r denotes a random number in the range of $[0, 1]$, l is a predefined parameter of value 1 or 2, while F_{C_i} is a value of objective fitness function for the selected carrion.

$$X_i = \begin{cases} X_i^{new, S1}, & F_i^{new, S1} < F_i \\ X_i, & otherwise \end{cases} \quad (43)$$

In Equation (43), $X_i^{new, S1}$ denotes the new position of the i th Tasmanian devil and $x_{i,j}^{new, S1}$ represents its value for the j th variable, while $F_i^{new, S1}$ represents its objective function value.

3.2.2. Feeding by Eating Prey (Exploitation Phase)

In this approach, there are two steps that the Tasmanian devil follows during attacking behavior. In the first step, it chooses the prey and launches an attack on it after scanning the surroundings. After reaching the prey, it chases it in the second step, to stop it from escaping and begin feeding. Therefore, the first step is designed in the same manner as that designed for the first approach of Tasmanian devil feeding. The process of choosing prey is mimicked in (44):

$$P_i = X_k, \quad i = 1, 2, 3, \dots, N, \quad k \in \{1, 2, \dots, N | k \neq i\} \quad (44)$$

where P_i denotes the prey selected by the i th Tasmanian devil. A new position for the Tasmanian devil in the search space is determined, based on the chosen prey. The updated location of the Tasmanian devil can be formulated using Equation (45).

$$x_{i,j}^{new, S2} = \begin{cases} x_{i,j} + r * (p_{i,j} - l * x_{i,j}), & F_{p_i} < F_i \\ x_{i,j} + r * (x_{i,j} - p_{i,j}), & otherwise \end{cases} \quad (45)$$

In Equation (45), $x_{i,j}$ represents the candidate value from the candidate solution for the j th variables, r denotes a random number in the range of $[0, 1]$, l is a predefined parameter of value 1 or 2, while F_{p_i} is a value of objective fitness function for the selected prey.

$$X_i = \begin{cases} X_i^{new, S2}, & F_i^{new, S2} < F_i \\ X_i, & otherwise \end{cases} \quad (46)$$

In Equation (46), $X_i^{new, S1}$ denotes the new position of the i th Tasmanian devil, $x_{i,j}^{new, S1}$ represents its value for the j th variable, and $F_i^{new, S1}$ represents its objective function value.

The second step during the attacking behavior demonstrated by the Tasmanian devil is the chasing process, which is designed using Equations (47)–(49). At this point, the Tasmanian devil's location is regarded as the hub of the area where the process of pursuing the prey is occurring. The Tasmanian devil follows its victim over a range that corresponds to this neighborhood's radius, which is computed using (47).

$$R = 0.01 \left(1 - \frac{t}{T} \right) \quad (47)$$

Here, R represents the attack location's immediate surroundings, t denotes the current iteration, and T represents the maximum number of iterations. A new position for the Tasmanian devil is determined, based on the chasing task. The updated location of the Tasmanian devil can be formulated using Equation (48).

$$x_{i,j}^{new} = x_{i,j} + (2 * r - 1) * R * x_{i,j} \quad (48)$$

$$X_i = \begin{cases} X_i^{new}, & F_i^{new} < F_i \\ X_i, & otherwise \end{cases} \quad (49)$$

In Equation (49), X_i^{new} denotes the new position of the i th Tasmanian devil in the district of X_i , $x_{i,j}^{new}$ represents its value for the j th variable, and F_i^{new} represents its objective function value. The flow chart of the TDO technique to address OADG in a DN is depicted in Figure 2; its explanation using pseudo code is presented in Algorithm A2 in the Appendix A section.

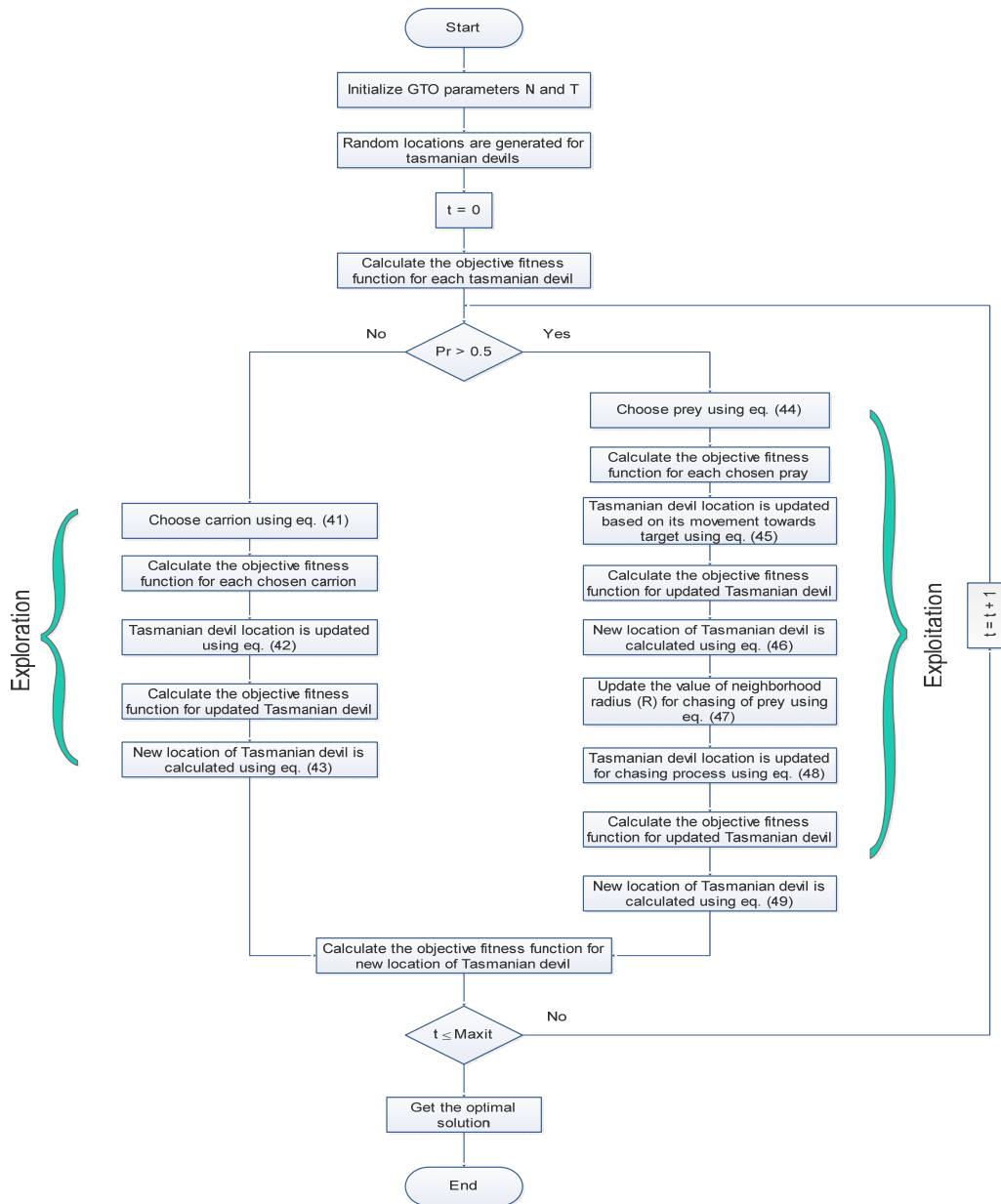


Figure 2. Flow chart of the TDO algorithm to solve the problem of OADG.

4. Simulation Results and Discussion

To evaluate the validity and effectiveness of the proposed algorithms, they have been implemented on two IEEE benchmark RDSs, including IEEE 33-bus and IEEE 69-bus systems, to optimize the SOF and MOF, while considering the CP load model as well as the VP load models, which consist of residential, commercial, and industrial load models. The reduction of APL and QPL by the optimal placement and sizing of DG units is accomplished by optimizing the SOF, while the minimization of APL, VD, and OCI and the maximization of VSI is simultaneously achieved by optimizing the MOF. The control parameter settings for the suggested methods are demonstrated in Table 3.

Table 3. Control parameter settings.

Algorithms	Parameters
GTO	population = 50, max-iter = 200, DG-size (MVA) = 0–2000, $\beta = 3$, $p = 0.03$, $W = 0.8$
TDO	population = 50, max-iter = 200, DG-size (MVA) = 0–2000

In this study, PV-DGs and WT-DGs are considered, PV-DGs having a unity pf while WT-DG has a combined pf (0.85). The period considered for this study is over 20 years. The proposed algorithms are simulated using MATLAB 2021b software and Windows 2010Pro, with Intel(R) Core (TM) i5-4210U CPU (2.4 GHz) and 8 GB of RAM. To verify the robustness of the algorithms, the following scenario and cases are considered for the studied systems:

Scenario 1: Optimizing SOF by integrating 3 DGs:

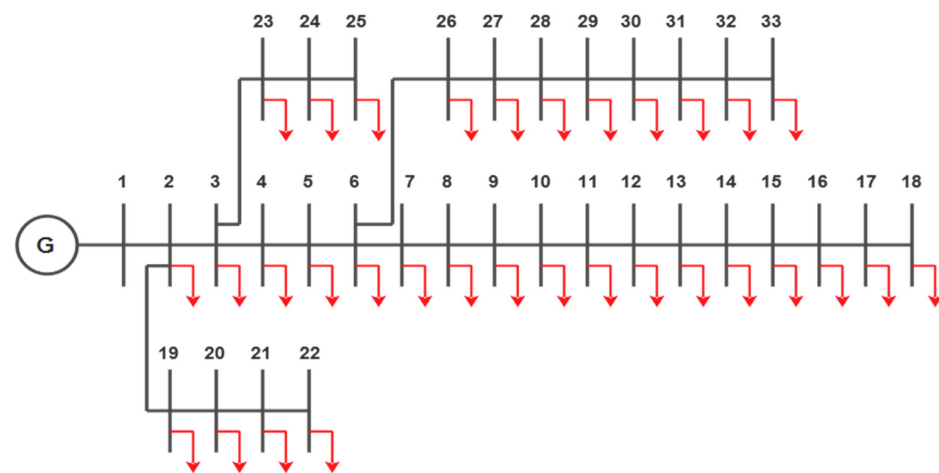
- Case 1: Minimizing APL for both CP and VP load models
- Case 2: Minimizing QPL for both CP and VP load models.

Scenario 2: Optimizing MOF by integrating 3 DGs:

- Case 1: Minimizing APL, VD, and OCI, and maximizing VSI for both CP and VP load models.

4.1. IEEE 33-Bus Test System

The proposed algorithms are first tested on a standard IEEE 33-bus RDS. A single-line diagram of the 33-bus RDS is shown in Figure 3. It consists of 33 buses and 32 branches, and the information about the line and load data of the system has been obtained from Ref. [61]. The total load demand of the system is $(3.715 + j2.300)$ MVA, with a base voltage and base MVA of 12.66 KV and 100 MVA, respectively.

**Figure 3.** Single-line diagram of a 33-bus RDS.

4.1.1. Scenario 1: Evaluation of a Single-Objective Function (SOF)

In this scenario, the TDO and GTO algorithms are used to solve the problem of the optimal placement and sizing of DGs, to reduce the total active and reactive power losses as SOFs for the CP load model and VP load model, i.e., industrial, residential, and commercial load models for three PV (unity pf) and three WT (0.85 pf).

CP Load Model

The total power loss of the system without the integration of DGs (the base case) is calculated by using the forward-backward power flow method, which is expressed as $(210.07 \text{ KW} + j142.44 \text{ KVAR})$. In the base case, active power loss and reactive power loss remain the same, while the losses are reduced as the number of DG units is increased in the

system. In the base case, the minimum voltage is 0.904 p.u. at bus 18, the voltage deviation is 0.1328 p.u., and the VSI is 0.6672 p.u. Table 4 represents the results of the OADG in the CP load model when used to optimize the SOF at unity pf (PV type). It can be seen from Table 4 that by using both the TDO and GTO algorithms, the total APL is reduced to 70.64 KW, which is a 66.37% reduction with respect to the base value. The results are compared with other existing optimization techniques. The result of the APL reduction is better than for the other BAT [50], SOS-NNA [57], IHHO [29], GAMS [10], CFA [21], and QOFBI [20] techniques mentioned in Table 4.

Likewise, the results of the OADG for APL minimization at 0.85 pf (WT type) are presented in Table 5. By employing the TDO and GTO algorithms, the APL is reduced to 14.39 KW, which is a 93.15% reduction, as can be seen in Table 4. The obtained results are compared with another optimization approach, I-DBEA [27]. The proposed algorithms yield better results in terms of APL reduction.

Moreover, the SOF is optimized to solve the problem of OADG with the integration of three PV (unity pf) and three WT (0.85 pf) for QPL minimization. The results and their discussion are presented in Tables A1 and A2 in Appendix A.

Table 4. Results comparison of the OADG for a 33-bus RDN for SOF (APL minimization) at unity pf (PV type) in a CP load model.

Methods	Location	DG Size (KW)	APL (KW) APLR (%)	VD (p.u.)	VSI (p.u.)
Base case	-	-	210.07	0.1328	0.6672
BAT [50]	13, 25, 30	380, 490, 990	72.78 (65.5)	-	0.8652
SOS-NNA [57]	13, 24, 30	801.8, 1091.3, 1053.6	72.7853 (65.5)	0.015113	1.1358
IHHO [29]	14, 24, 30	775.54, 1080.83, 1066.69	72.79 (65.50)	-	-
GAMS [10]	14, 24, 30	770.9, 1096.9, 1065.8	72.79 (65.50)	-	-
CFA [21]	30, 24, 13	1059.32, 1090.16, 801.88	72.79 (65.50)	-	-
QOFBI [20]	24, 30, 13	1091.33, 1053.64, 801.71	72.78 (65.5)	-	-
TDO [P]	30, 14, 24	1213, 866, 1186	70.64 (66.37)	0.011541	0.8940
GTO [P]	24, 30, 14	1186, 1213, 866	70.64 (66.37)	0.011541	0.8940

Table 5. Results comparison of OADG for a 33-bus RDN for the SOF (with APL minimization) at 0.85 pf (WT type) in the CP load model.

Methods	Location	DG Size		APL (KW) APLR (%)	VD (p.u.)	VSI (p.u.)
		KW	KVAR			
Base case	-	-	-	210.07	0.1328	0.6672
I-DBEA [27]	13, 24, 30	749.1, 1042, 1239.5	-	14.57 (92.81)	0.0002	0.9733
TDO [P]	30, 24, 13	1333, 1147, 836	826, 640, 486	14.39 (93.15)	0.000604	0.9669
GTO [P]	24, 30, 13	1147, 1333, 836	640, 826, 486	14.39 (93.15)	0.000604	0.9669

VP Load Model

This section extends the OADG issue for practical non-linear loads to show how strongly power demands rely on the voltage of the network. In the base case, the APL for industrial load models is 163.22 KW, for residential load models, it is 158.76 KW, and for commercial load models, it is 152.32 KW. Table 6 shows the results of the SOF based on APL minimization for the optimum placement and sizing of DGs at unity pf (PV-type). It can be seen from the table that by employing the TDO and GTO algorithms, APL is reduced to 34.55 KW (78.83%) for industrial, 42.05 KW (73.51%) for residential, and 44.80 KW (70.59%) for commercial load models. The results are compared with another optimization method, BAT [50], as mentioned in Table 6. The results obtained by employing the proposed algorithms are better in terms of APL reduction.

Table 6. Results comparison of OADG for 33 bus RDN for the SOF (APL minimization) at unity pf (PV type) in the VP load model.

Methods	Parameters	Industrial	Residential	Commercial
Base case	APL (KW)	163.22	158.76	152.32
	VD (p.u.)	0.098637	0.097821	0.094018
	VSI (p.u.)	0.70741	0.70953	0.71526
BAT [50]	Location	13, 25, 30	13, 25, 30	13, 25, 30
	DG size (KW)	790, 850, 1020	720, 830, 980	710, 820, 940
	APL (KW)	36.01	43.70	46.42
	APLR (%)	77.99	72.53	69.57
	VD (p.u.)	-	-	-
	VSI (p.u.)	0.9069	0.8974	0.8959
TDO [P]	Location	14, 24, 30	24, 30, 14	24, 30, 14
	DG size (KW)	843, 1187, 1163	1158, 1108, 793	1132, 1065, 756
	APL (KW)	34.55	42.05	44.80
	APLR (%)	78.83	73.51	70.59
	VD (p.u.)	0.005841	0.007153	0.007595
	VSI (p.u.)	0.9245	0.9164	0.9139
GTO [P]	Location	14, 24, 30	24, 14, 30	30, 24, 14
	DG size (KW)	843, 1187, 1163	1158, 793, 1108	1064, 1136, 755
	APL (KW)	34.55	42.05	44.80
	APLR (%)	78.83	73.51	70.59
	VD (p.u.)	0.005841	0.007152	0.007599
	VSI (p.u.)	0.9245	0.9164	0.9139

Likewise, Table 7 represents the results of the OADG at 0.85 pf (WT type) for APL minimization with different load models. The APL is reduced to 10.53 KW (93.55%), 10.38 KW (93.46%), and 10.33 KW (93.22%) for the industrial, residential, and commercial load models, respectively, for both the TDO and GTO algorithms. It can be concluded that the APL minimization is at maximum for the industrial load models for PV (unity pf).

Table 7. Results of the OADG for a 33-bus RDN for SOP (APL minimization) at 0.85 pf (WT type) in the VP load model.

Parameters	0.85 pf (WT Type)			
	Industrial	Residential	Commercial	
Base case	APL (KW)	163.22	158.76	152.32
	VD (p.u.)	0.098637	0.097821	0.094018
	VSI (p.u.)	0.70741	0.70953	0.71526
TDO [P]	APL (KW)	10.53	10.38	10.33
	APLR (%)	93.55	93.46	93.22
	Location	24, 13, 30	30, 13, 24	30, 24, 13
	DG Size (KW)	1181, 869, 1129	1137, 798, 1139	1123, 1111, 750
	DG Size (KVAR)	477, 250, 700	704, 321, 531	696, 553, 349
	DG Size (KVA)	3484	3445	3385
	VD (p.u.)	0.000517	0.000507	0.000486
	VSI (p.u.)	0.9694	0.9698	0.9705
GTO [P]	APL (KW)	10.53	10.38	10.33
	APLR (%)	93.55	93.46	93.22
	Location	24, 13, 30	24, 13, 30	30, 24, 13
	DG Size (KW)	1182, 868, 1129	1140, 798, 1137	1123, 1111, 750
	DG Size (KVAR)	477, 249, 700	532, 321, 705	696, 553, 350
	DG Size (KVA)	3484	3447	3385
	VD (p.u.)	0.000516	0.000505	0.000486
	VSI (p.u.)	0.9694	0.9698	0.9705

Furthermore, the study has been expanded to solve the problem of the optimal allocation of DGs for reactive power loss minimization (QPL) for VP load models, with the integration of three PV (unity pf) and three WT (0.85 pf). The results of the QPL minimization and a discussion of the findings are presented in Tables A3 and A4 in Appendix A.

Voltage Profiles for 33 Bus RDS

Figure 4 illustrates the impact of the installation of various types of DGs on the voltage profile for a 33-bus RDS under various types of loads, i.e., constant, residential, commercial, and industrial load models. In Figure 4, “Const” stands for constant, “Res” denotes residential, “Comm” denotes commercial, and “Ind” denotes industrial load models. The outer values of the graphs represent the “bus number” and the inner values represent “bus voltage”, corresponding to the particular bus number.

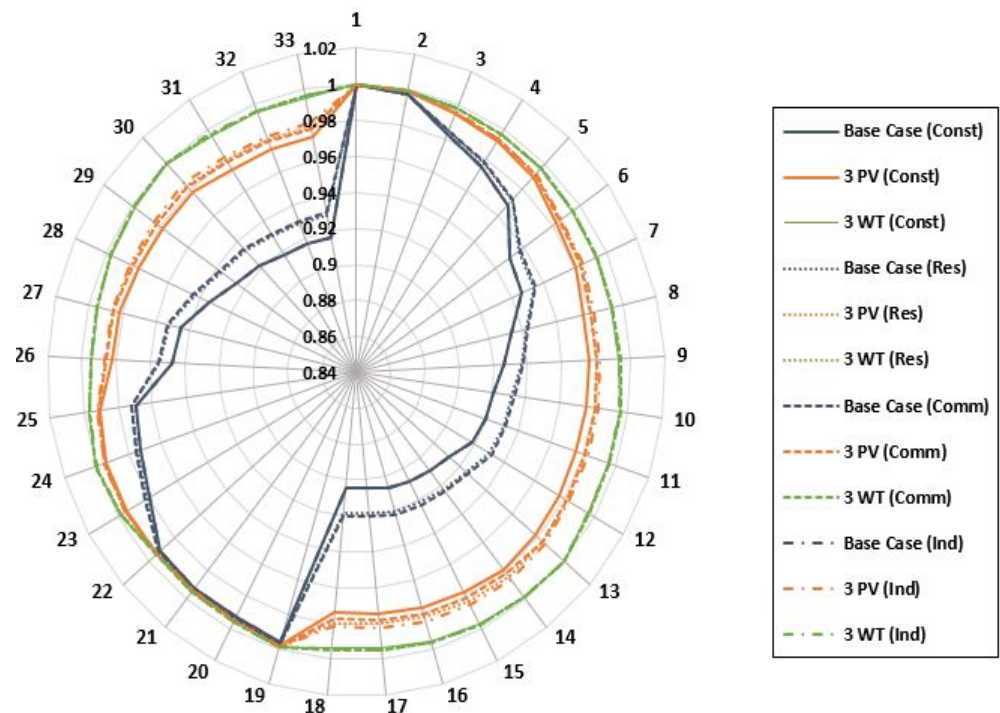


Figure 4. Voltage profiles for an IEEE 33-bus system for different loads in different cases for scenario 1.

Active Power Losses for a 33-Bus RDS

Figure 5 depicts the APL information for each bus of a 33-bus RDS after the integration of three PV (unity pf) and three WT (0.85 pf) under various types of loads, i.e., constant, residential, commercial, and industrial loads, under scenario 1.

Convergence Characteristics for a 33-Bus RDS

Figure 6a,b displays the convergence characteristics of the GTO and TDO algorithms at various power factors (unity and 0.85) for the CP load model. It is apparent from the figure below that the GTO algorithm has a higher efficiency than the TDO algorithm.

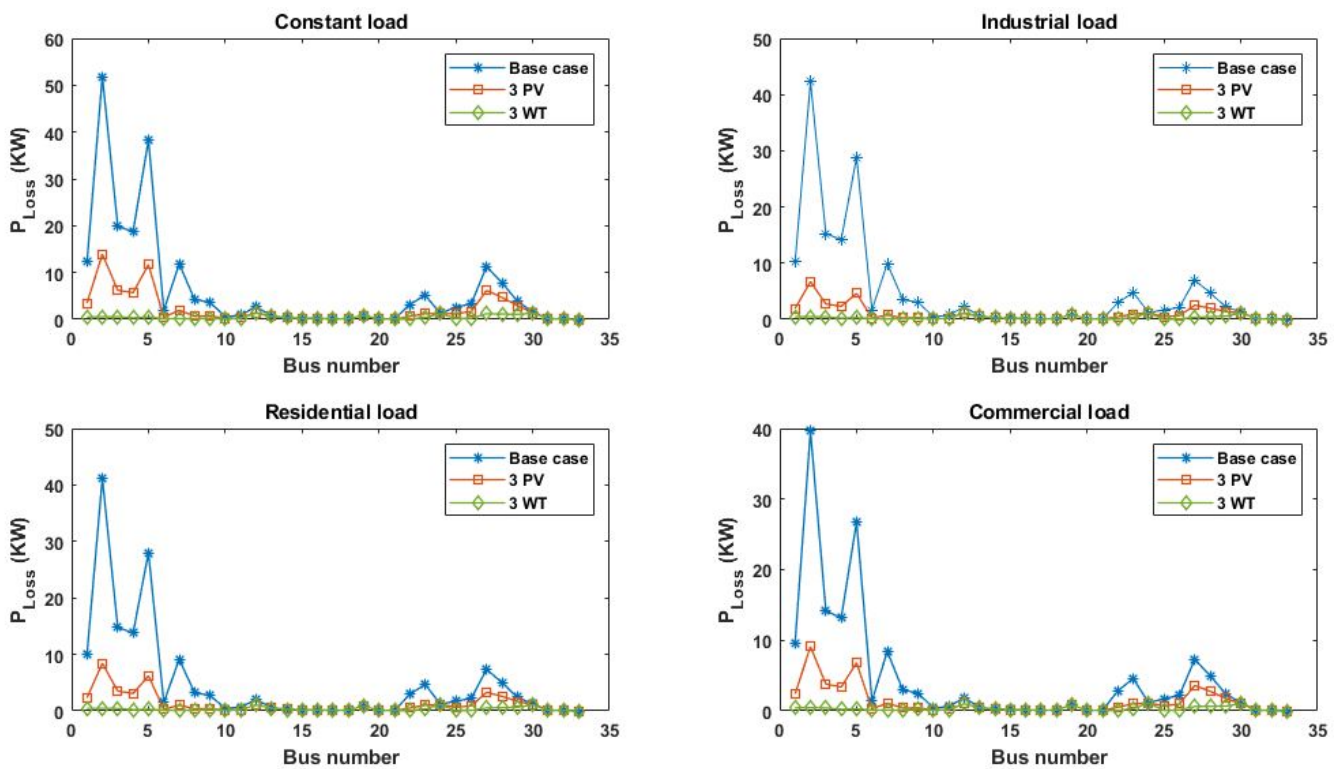


Figure 5. Active power loss for a 33-bus RDS for various types of loads, under scenario 1.

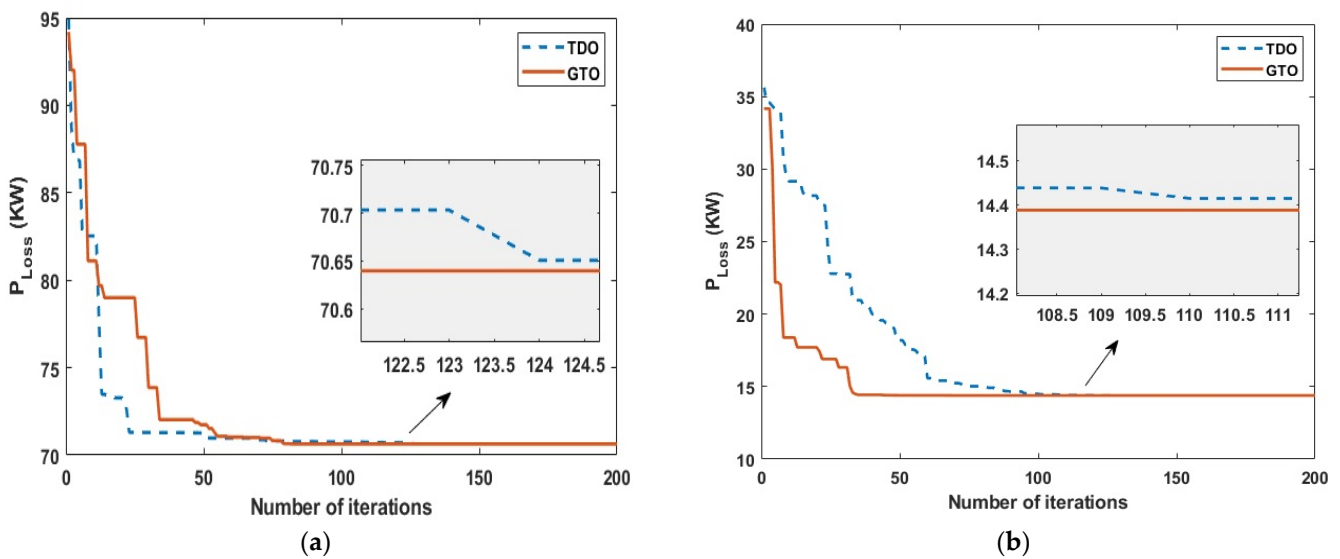


Figure 6. Convergence characteristics of the TDO and GTO algorithms for an IEEE 33-bus system under scenario 1 at different pf; (a) unity pf (b) 0.85 pf.

4.1.2. Evaluation of Multi-Objective Function (MOF)

In this scenario, the TDO and GTO algorithms are employed to optimize the MOF, based on APL, VD, VSI, and OCI, to solve the problem of OADG in RDS, considering the CP load model and VP load models for three PV (unity pf) and three WT (0.85 pf).

CP Load Model

The total power loss of the system in the base case is (210.07KW + j142.44KVAR), the VD is 0.1328 p.u., VSI is 0.6672, and the operating cost is 16.837972 million USD (M\$). Table 8 presents the results of the MOF in terms of APL reduction, VD minimization, VSI

maximization, and the minimization of an operating costs index for the optimum placement and sizing of DGs for three PV (unity pf) and three WT (0.85 pf) for the CP load model.

Table 8. Results of OADG for a 33-bus RDN for MOF in the CP load model.

Parameters	Base Case	Unity pf (PV Type)		0.85 pf (WT Type)	
		TDO [P]	GTO [P]	TDO [P]	GTO [P]
APL (KW)	210.07	71.74	72.02	14.65	14.66
APLR (%)	-	65.85%	65.72%	93.03%	93.02%
Location	-	30, 24, 14	14, 30, 24	13, 30, 24	13, 30, 24
DG Size (KW)	-	1371, 1282, 913	922, 1393, 1273	884, 1368, 1205	874, 1367, 1239
DG Size (KVAR)	-	-	-	504, 848, 660	509, 847, 643
DG Size (KVA)	-	3566	3588	4000	4013
VD (p.u.)	0.1328	0.007390	0.006894	0.000287	0.000291
VSI (p.u.)	0.6672	0.9160	0.9189	0.9753	0.9753
OC _{DG} (M\$)	16.837972	0.946949	0.853764	1.169609	1.071008
DG _M (M\$)	-	2.185373	2.198856	2.118574	2.132669
DG _O (M\$)	-	9.053689	9.109545	8.776950	8.835345
DG _{IC} (M\$)	-	1.4264	1.4352	1.3828	1.3920
OC _{TDG} (M\$)	16.837972	13.612412	13.597365	13.447933	13.431022
OCI	1.0	0.8084	0.8075	0.7987	0.7977

Note: (M\$)—Million USD.

It can be seen from the table that at unity pf (PV type), the APL is reduced to 71.74 KW (65.85%) for the TDO algorithm and 72.02 KW (65.72%) for the GTO algorithm. The VD obtained by employing the TDO and GTO algorithms is 0.007390 p.u. and 0.006894 p.u., respectively, while the value of VSI computed for the TDO and GTO algorithms is 0.9160 p.u. and 0.9189 p.u., respectively; the operating cost index for both the TDO and GTO algorithms is 8084 and 8075, respectively. Furthermore, the cost savings after 20 years at unity pf (PV-type) are 19.16% and 19.25% for the GTO and TDO algorithms, respectively.

Similarly, at 0.85 pf (WT type), the APL is reduced to 14.65 KW (93.03%) for the TDO algorithm and 14.66 KW (93%) for the GTO algorithm. The VD obtained by employing the GTO and TDO algorithms is 0.000287 p.u. and 0.000291 p.u., respectively, while the value of VSI computed for both the TDO and GTO algorithms is 0.9753 p.u., and the operating cost index for the TDO and GTO algorithms is 7987 and 7977, respectively. Moreover, the cost savings after 20 years at 0.85 pf (WT type) for the TDO and GTO algorithms are 20.13% and 20.23%, respectively.

It can be concluded that the results obtained at 0.85 pf (WT type) in terms of APL reduction, the minimization of VD, the minimization of OCI, and the maximization of VSI are improved compared to the results obtained at unity pf (PV type). Furthermore, the cost saving is at a maximum, at 0.85 pf (PV type).

VP Load Model

The results of MOF in terms of APL reduction, VD minimization, VSI maximization, and the minimization of the operating cost index for the optimum placement and sizing of DGs for VP load models for three PV (unity pf) and three WT (0.85 pf) are shown in Tables 9 and 10.

Table 9. Results of the OADG for a 33-bus RDN for MOF at unity pf (PV Type) in a VP load model.

Parameters		Unity pf (PV Type)					
		Industrial		Residential		Commercial	
Base case	APL (KW)	163.22		158.76		152.32	
	VD (p.u.)	0.098637		0.097821		0.094018	
	VSI (p.u.)	0.70741		0.70953		0.71526	
	OC (M\$)	16.484648		15.859454		15.371032	
Parameters		TDO [P]	GTO [P]	TDO [P]	GTO [P]	TDO [P]	GTO [P]
With 3 DGs	APL (KW)	35.09	35.09	42.69	42.70	45.50	45.50
	APLR (%)	78.50%	78.50%	73.11%	73.10%	70.13%	70.13%
	Location	14, 30, 24	24, 30, 14	14, 24, 30	14, 24, 30	30, 14, 24	24, 13, 30
	DG Size (KW)	893, 1255, 1261	1257, 1256, 894	829, 1224, 1230	827, 1231, 1232	1199, 1197, 788	1199, 843, 1161
	DG Size (KVAR)	-	-	-	-	-	-
	DG Size (KVA)	3409	3407	3283	3290	3184	3203
	VD (p.u.)	0.00374	0.00373	0.00472	0.00472	0.00498	0.00485
	VSI (p.u.)	0.9385	0.9386	0.9331	0.9333	0.9319	0.9302
	OC _{DG} (M\$)	1.310889	1.319478	1.277943	1.24798	1.253954	1.172408
	DG _M (M\$)	2.089158	2.087932	2.011941	2.016231	1.951270	1.962914
	DG _O (M\$)	8.655083	8.650005	8.335183	8.352955	8.083833	8.132071
	DG _{IC} (M\$)	1.3636	1.3628	1.3132	1.316	1.2736	1.2812
	OC _{TDG} (M\$)	13.418730	13.420216	12.938267	12.933171	12.562656	12.548593
	OCI	0.8141	0.8141	0.8158	0.8155	0.8173	0.8164

Table 10. Results of OADG for a 33-bus RDN for MOF at 0.85 pf (WT type) with a VP load model.

Parameters		0.85 pf (WT Type)					
		Industrial		Residential		Commercial	
Base case	APL (KW)	163.22		158.76		152.32	
	VD (p.u.)	0.098637		0.097821		0.094018	
	VSI (p.u.)	0.70741		0.70953		0.71526	
	OC (M\$)	16.484648		15.859454		15.371032	
Parameters		TDO [P]	GTO [P]	TDO [P]	GTO [P]	TDO [P]	GTO [P]
With 3 DGs	APL (KW)	10.69	10.69	10.50	10.51	10.44	10.45
	APLR (%)	93.45%	93.45%	93.39 %	93.38%	93.15%	93.14%
	Location	30, 24, 13	30, 24, 13	30, 24, 13	13, 24, 30	13, 30, 24	30, 24, 13
	DG Size (KW)	1151, 1255, 901	1160, 1258, 894	1160, 1200, 824	831, 1204, 1157	769, 1149, 1166	1151, 1170, 771
	DG Size (KVAR)	706, 484, 265	708, 489, 267	719, 531, 337	331, 532, 717	365, 712, 539	713, 544, 360
	DG Size (KVA)	3613	3621	3558	3562	3482	3489
	VD (p.u.)	0.000291	0.000288	0.000294	0.000294	0.000294	0.000293
	VSI (p.u.)	0.9755	0.9756	0.9755	0.9755	0.9755	0.9756
	OC _{DG} (M\$)	1.643765	1.622348	1.564572	1.530298	1.532499	1.498209
	DG _M (M\$)	2.026649	2.029713	1.951270	1.956173	1.889986	1.894889
	DG _O (M\$)	8.396116	8.408811	8.083833	8.104144	7.829943	7.850254
	DG _{IC} (M\$)	1.3228	1.3248	1.2736	1.2768	1.2336	1.2368
	OC _{TDG} (M\$)	13.389330	13.385671	12.873275	12.867414	12.486029	12.480152
	OCI	0.8122	0.8120	0.8117	0.8113	0.8123	0.8119

It can be seen from Table 9 that at unity pf (PV type), by employing the TDO algorithm, the APL is reduced to 35.09 KW (78.50%) for the industrial load model, 42.69 KW (73.11%) for the residential load model, and 45.50 KW (70.11%) for the commercial load model, while by employing the GTO algorithm, the reduction in APL for industrial load is 35.09 KW

(78.50%), for residential load, it is 42.70 KW (73.10%), and for commercial load, it is 45.50 KW (70.13%). The obtained VD from the TDO algorithm for the industrial load model is 0.00374 p.u., for the residential load model, it is 0.00472 p.u., and for the commercial load model, it is 0.00498 p.u., while the VD obtained from the GTO algorithm is 0.00373 p.u., for the industrial load model, 0.00472 p.u. for the residential load model, and 0.00485 p.u. for the commercial load model. The VSI that has been computed for the industrial load model is 0.9385 p.u., for the residential load model it is 0.9331 p.u., and for the commercial load model, it is 0.9319 p.u., established by employing the TDO algorithm, while by employing the GTO algorithm, the VD for the industrial load model is 0.9386 p.u., for the residential load model, it is 0.9333 p.u., and for the commercial load model, it is 0.9302 p.u. The operating cost index obtained from the TDO and GTO algorithms for an industrial load is 0.8141, for a residential load it is 0.8158 and 0.8155, and for a commercial load, it is 0.8173 and 0.8164, respectively. Besides this, the cost saving after 20 years for the industrial load will be 18.59% for both the TDO and GTO algorithms, for a residential load, it will be 18.42% and 18.45% for the TDO and GTO algorithms, and for a commercial load, it will be 18.27% and 18.36% for the TDO and GTO algorithms.

Moreover, the results of the OADG for MOF at 0.85 pf (WT type) are shown in Table 10. By employing TDO, the APL is reduced to 10.69 KW (93.45%) for the industrial load model, to 10.50 KW (93.39%) for the residential load, and 10.44 KW (93.15%) for the commercial load, while by employing the GTO algorithm, the APL is reduced to 10.69 KW (93.45%), 10.51 KW (93.38%), and 10.45 KW (93.14%) for industrial, residential, and commercial load models, respectively. The obtained VD from the TDO algorithm for industrial, residential, and commercial models is 0.000291 p.u., 0.000294 p.u., and 0.000294 p.u., respectively, while the VD obtained from the GTO algorithm is 0.000288 p.u. for industrial load, 0.000294 p.u. for residential load, and for commercial load, it is 0.000293 p.u. The VSI that was computed by employing the TDO algorithm for the industrial load model is 0.9755 p.u., for the residential model, it is 0.9755 p.u., and for the commercial model, it is 0.9755 p.u., while by employing the GTO algorithm, the VSI computed for the industrial load model is 0.9756 p.u., for the residential model it is 0.9755 p.u., and for the commercial load model, it is 0.9756 p.u. The operating cost index obtained from the TDO and GTO algorithms for industrial load is 0.8122 and 0.8120, for residential load, it is 0.8117 and 0.8113, and for commercial load, it is 0.8123 and 0.8119, respectively.

Besides this, the cost saving after 20 years for an industrial load will be 18.78% and 18.80% for the TDO and GTO algorithms, for a residential load, 18.83% and 18.87% for the TDO and GTO algorithms, and for a commercial load, it will be 18.77% and 18.81% for the TDO and GTO algorithms.

It can be concluded that compared to unity pf (PV type), the results of the MOF in terms of APL reduction, the minimization of VD and OCI, and the maximization of VSI are improved at 0.85 pf (WT type). Furthermore, the maximum cost saving is achieved at 0.85 pf (WT type) for industrial, residential, and commercial load models.

4.2. IEEE 69-Bus Test System

In this section, the conclusions of standard IEEE 69-bus RDSs are achieved by the suggested techniques. Figure 7 displays a 69-bus DS single-line diagram. It has 69 buses and 68 branches, and the information about the line and load data of the system has been obtained from Ref. [62]. The base voltage and base MVA of the system are 12.66 KV and 100 MVA, respectively, while the total load demand is $(3.8 + j2.69)$ MVA.

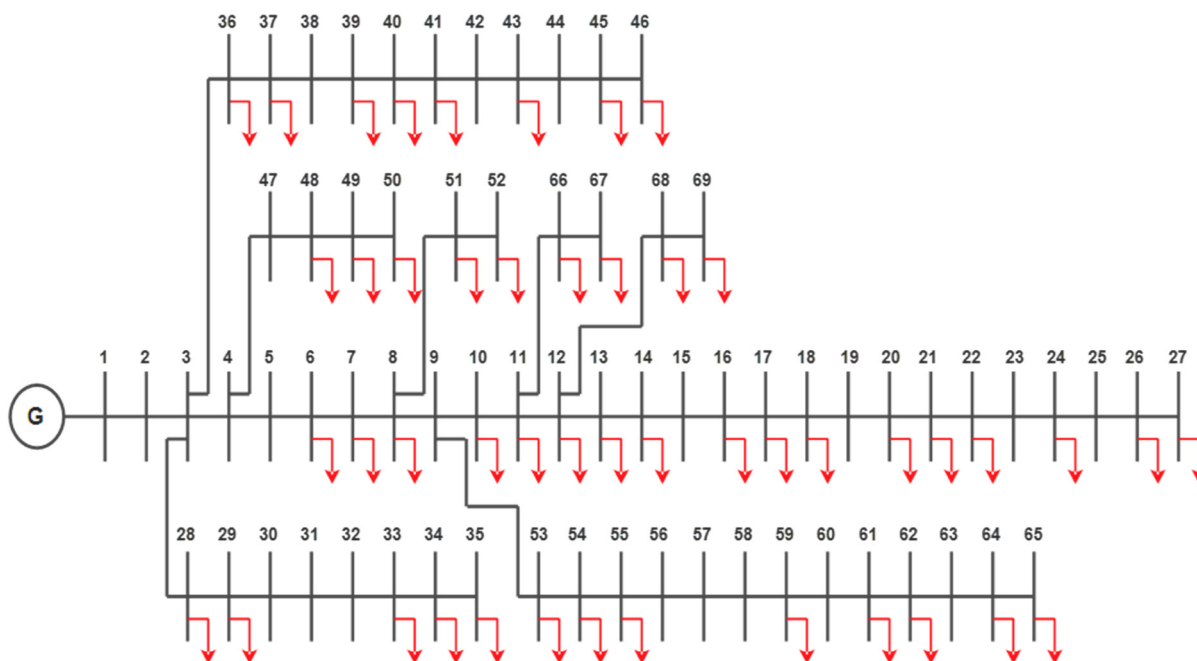


Figure 7. Single-line diagram of a 69-bus RDS.

4.2.1. Scenario 1: Evaluation of a Single-Objective Function (SOF)

In this scenario, the TDO and GTO algorithms are used to solve the problem of the optimal allocation of DGs in a distribution network to reduce the total active and reactive power losses as the SOF for a CP load model and VP load models, i.e., industrial, residential, and commercial load models for three PV (unity pf) and three WT (0.85 pf).

CP Load Model

The forward-backward load flow method is used to determine a power flow solution. The total power loss of the system in the base case is (225.60KW + j101.99KVAR) and the minimum voltage is 0.9102 p.u. at bus 65. The VD and VSI in the base case are 0.09803 p.u. and 0.6855 p.u., respectively. The results of the proposed algorithms for OADG at unity pf (PV type) in the CP load model are presented in Table 11. It can be seen from the table that the total APL is reduced to 68.68 KW for both the TDO and GTO algorithms, that is, a 69.42% reduction with respect to the base value. The obtained results are compared with other optimization approaches, BAT [50], SOS-NNA [57], IHHO [29], I-DBEA [27], and QOFBI [20], and are presented in the table. The proposed algorithms performed well in terms of APL reduction.

Table 11. Results comparison of OADG for a 69-bus RDN for SOF (APL minimization) at unity pf (PV type) in the CP load model.

Methods	Location	DG Size (KW)	APL (KW) APLR (KW)	VD (p.u.)	VSI (p.u.)
Base case	-	-	224.60	0.09803	0.68548
BAT [50]	12, 19, 61	535, 340, 1693	68.97 (69.34)	-	0.9113
SOS-NNA [57]	11, 18, 61	526.8, 380.3, 1719	69.4284 (69.14)	0.005201	1.0887
IHHO [29]	11, 17, 61	527.2, 382.5, 1719.4	69.41 (69.15)	-	-
QOFBI [20]	11, 61, 18	526.8, 1718.97, 380.06	69.3972 (69.15)	-	-
I-DBEA [27]	61, 19, 11	2148.7, 471.7, 712.6	78.347 (65.17)	0.0002	0.9772
TDO [P]	18, 61, 11	431, 1931, 525	68.68 (69.42)	0.003613	0.9356
GTO [P]	11, 18, 61	525, 431, 1931	68.68 (69.42)	0.003613	0.9356

Likewise, the results of OADG for APL minimization at 0.85 pf (WT type) are presented in Table 12. By employing the TDO and GTO algorithms, the APL is reduced to 7.03 KW, which is a 96.87% reduction; this is better than the other optimization approach, I-DBEA [27], as mentioned in Table 12.

Table 12. Results comparison of OADG for a 69-bus RDN for the SOF (APL minimization) at 0.85 pf (WT type) with a CP load model.

Methods	Location	DG Size		APL (KW) APLR (%)	VD (p.u.)	VSI (p.u.)
		KW	KVAR			
Base case	-	-	-	224.60	0.09803	0.68548
I-DBEA [27]	61, 59, 16	1500, 370, 575	-	7.966 (96.45)	0.000266	0.9774
TDO [P]	18, 61, 11	428, 1700, 687	265, 1054, 426	7.03 (96.87%)	0.000718	0.9587
GTO [P]	61, 18, 11	1700, 429, 689	1054, 266, 427	7.03 (96.87%)	0.000711	0.9588

Moreover, the SOF is optimized to solve the problem of OADG with the integration of three PV (unity pf) and three WT (0.85pf) for QPL minimization. The results and a discussion of the findings are presented in Tables A5 and A6 in Appendix A.

VP Load Model

This section extends the OADG issue for practical non-linear load models to show how strongly power demands rely on the voltage of the network. In the base case, the APL for an industrial load model is 171.72KW, for a residential load model, it is 165.31KW, and for a commercial load model, it is 157.39 KW. Table 13 shows the results of the SOF based on APL minimization for the optimum placement and sizing of DGs at unity pf (PV-type). It can be seen from the table that the APL is reduced to 28.71 KW (83.28%), 37.61 KW (77.25%), and 41.07 KW (73.91%) for industrial, residential, and commercial load models, respectively, for both the TDO and GTO algorithms. The obtained results are compared with another optimization method, BAT [50], as mentioned in Table 13. The proposed algorithms show better results in terms of APL reduction.

Table 13. Comparative results of OADG for a 69-bus RDN for the SOF (APL minimization) at unity pf (PV Type) in a VP load model.

Methods	Parameters	Industrial	Residential	Commercial
Base case	APL (KW)	171.7224	165.3079	157.3927
	VD (p.u.)	0.079855	0.076462	0.072316
	VSI (p.u.)	0.71505	0.7218	0.72986
BAT [50]	Location	12, 19, 61	12, 19, 61	12, 19, 61
	DG size (KW)	460, 320, 1670	450, 310, 1570	440, 300, 1480
	APL (KW)	28.81	37.73	41.33
	APLR (%)	83.19	77.11	73.66
	VD (p.u.)	-	-	-
	VSI (p.u.)	0.9431	0.9357	0.9314
TDO [P]	Location	61, 11, 18	18, 61, 11	11, 61, 18
	DG size (KW)	1854, 543, 422	421, 1761, 424	517, 1656, 410
	APL (KW)	28.71	37.54	41.07
	APLR (%)	83.28	77.29	73.91
	VD (p.u.)	0.002009	0.002428	0.002575
	VSI (p.u.)	0.9523	0.9477	0.9463
GTO [P]	Location	18, 11, 61	18, 11, 61	18, 11, 61
	DG size (KW)	424, 538, 1855	412, 523, 1748	402, 512, 1663
	APL (KW)	28.71	37.54	41.07
	APLR (%)	83.28	77.29	73.91
	VD (p.u.)	0.00201	0.002429	0.002575
	VSI (p.u.)	0.9523	0.9477	0.9463

Likewise, Table 14 represents the results of the OADG at 0.85 pf (WT type) for APL minimization for the different load models. The APL is reduced to 3.89 KW (97.73) for the industrial load model, to 3.87 KW (97.66%) for the residential load model, and for a commercial load model, it is reduced to 3.83 KW (97.57%) for both the TDO and GTO algorithms.

Table 14. Results of the OADG for a 69-bus RDN for the SOF (APL minimization) at 0.85 pf (WT Type) in a VP load model.

Parameters		0.85 pf (WT Type)		
		Industrial	Residential	Commercial
Base case	APL (KW)	171.7224	165.3079	157.3927
	VD (p.u.)	0.079855	0.076462	0.072316
	VSI (p.u.)	0.71505	0.7218	0.72986
TDO [P]	APL (KW)	3.89	3.87	3.83
	APLR (%)	97.73	97.66	97.57
	Location	11, 17, 61	11, 61, 18	61, 18, 11
	DG Size (KW)	546, 418, 1830	544, 1711, 402	1628, 400, 517
	DG Size (KVAR)	329, 217, 777	337, 927, 239	988, 248, 318
	DG Size (KVA)	3091	3052	2982
	VD (p.u.)	0.000118	0.000118	0.000118
	VSI (p.u.)	0.9778	0.9777	0.9777
GTO [P]	APL (KW)	3.89	3.87	3.82
	APLR (%)	97.73	97.66	97.57
	Location	11, 61, 18	18, 61, 11	61, 11, 18
	DG Size (KW)	546, 1830, 418	403, 1712, 542	1622, 539, 394
	DG Size (KVAR)	329, 777, 217	239, 927, 336	983, 334, 244
	DG Size (KVA)	3091	3052	2994
	VD (p.u.)	0.000118	0.000118	0.000116
	VSI (p.u.)	0.9778	0.9777	0.9777

Moreover, the study has been expanded to solve the problem of the optimal allocation of DGs for reactive power loss minimization (QPL) for VP load models, with the integration of three PV (unity pf) and three WT (0.85 pf). The results of the QPL minimization and a discussion of the findings are presented in Tables A7 and A8 in Appendix A.

Voltage Profiles for a 69-Bus RDS

Figure 8 illustrates the impact of the installation of various types of DGs on the voltage profile for a 33-bus RDS under various types of loads, i.e., constant, residential, commercial, and industrial load models. In Figure 8, “Const” stands for constant, “Res” denotes the residential load, “Comm” denotes the commercial load, and “Ind” stands for the industrial load. The outer values of the graphs represent the “bus number” and the inner values represent the “bus voltage” corresponding to the particular bus number.

Active Power Losses for a 69-Bus RDS

Figure 9 depicts the active power loss information for each bus of a 33-bus RDS after the integration of three PV (unity pf) and three WT (0.85 pf), under various types of loads, i.e., constant, residential, commercial, and industrial loads, under scenario 1.

Convergence Characteristics for 69 Bus RDS

Figure 10a,b displays the convergence characteristics of the GTO and TDO algorithms at various power factors (unity and 0.85) for the CP load model. It is apparent from the figure that the GTO algorithm has higher efficiency than the TDO algorithm.

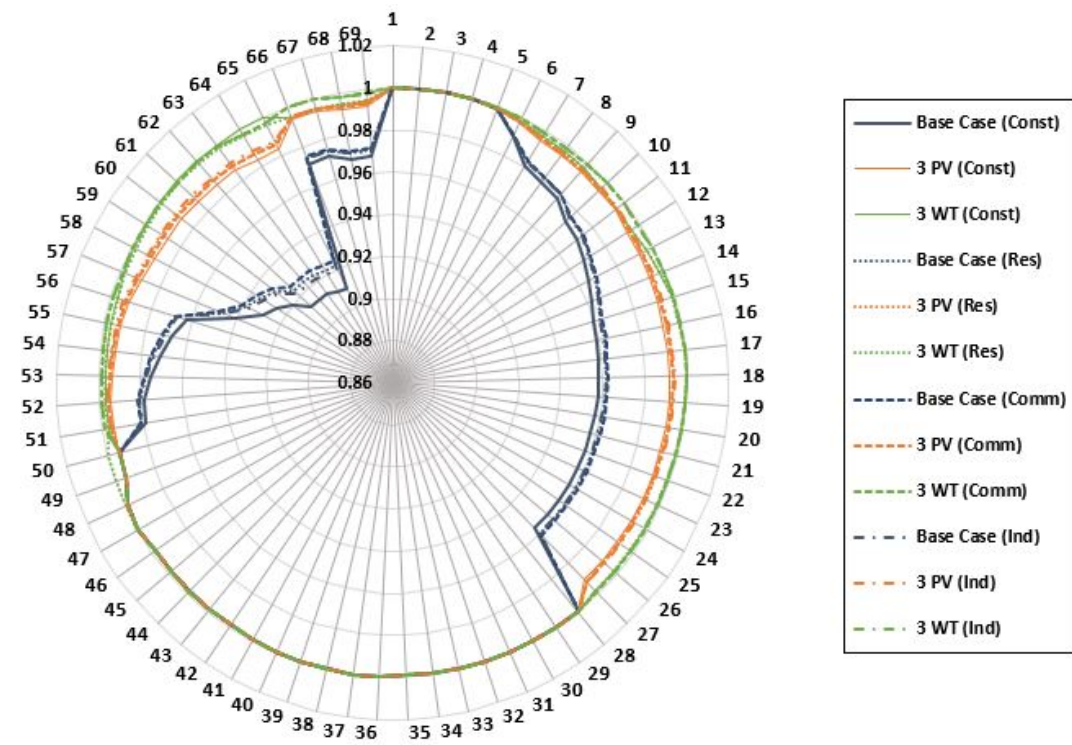


Figure 8. Voltage profiles for an IEEE 69-bus system for different loads at different cases in scenario 1.

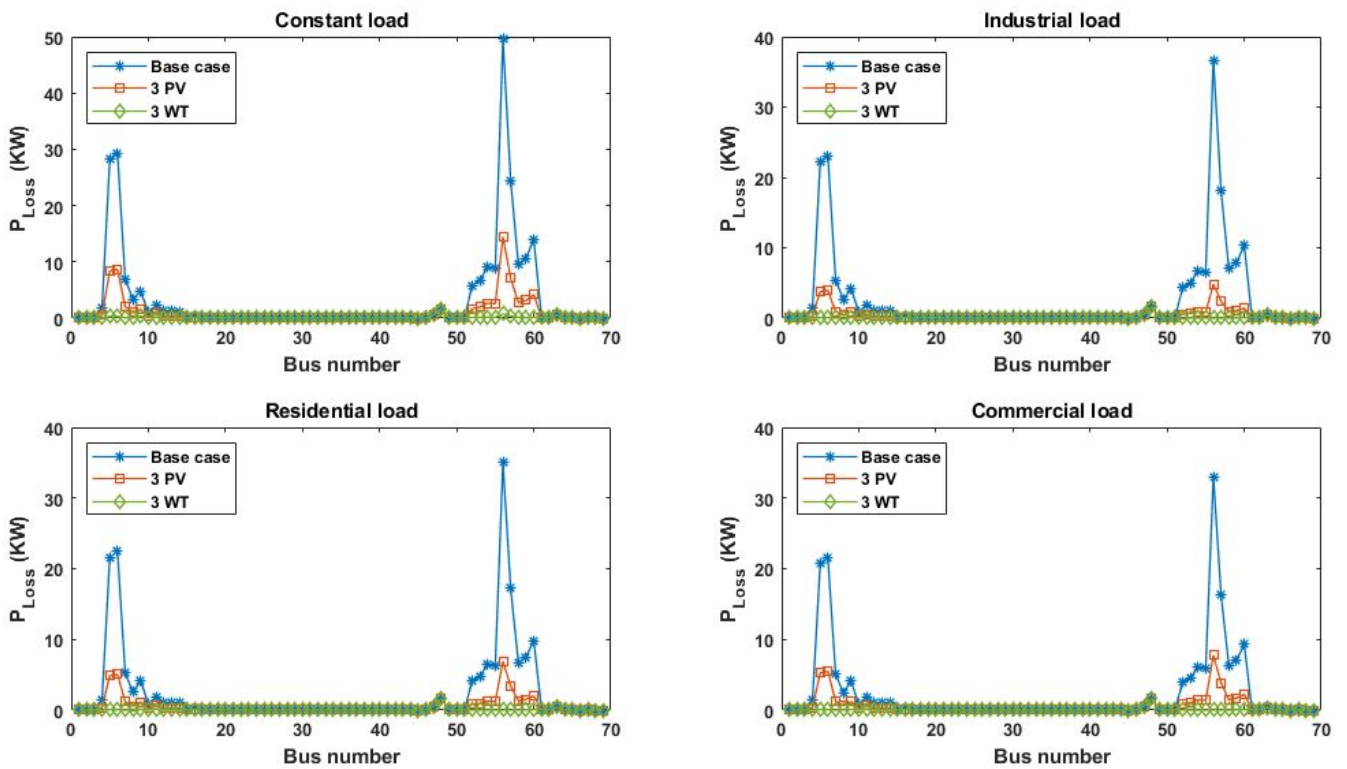


Figure 9. Active power loss for 69 buses under various types of loads for scenario 1.

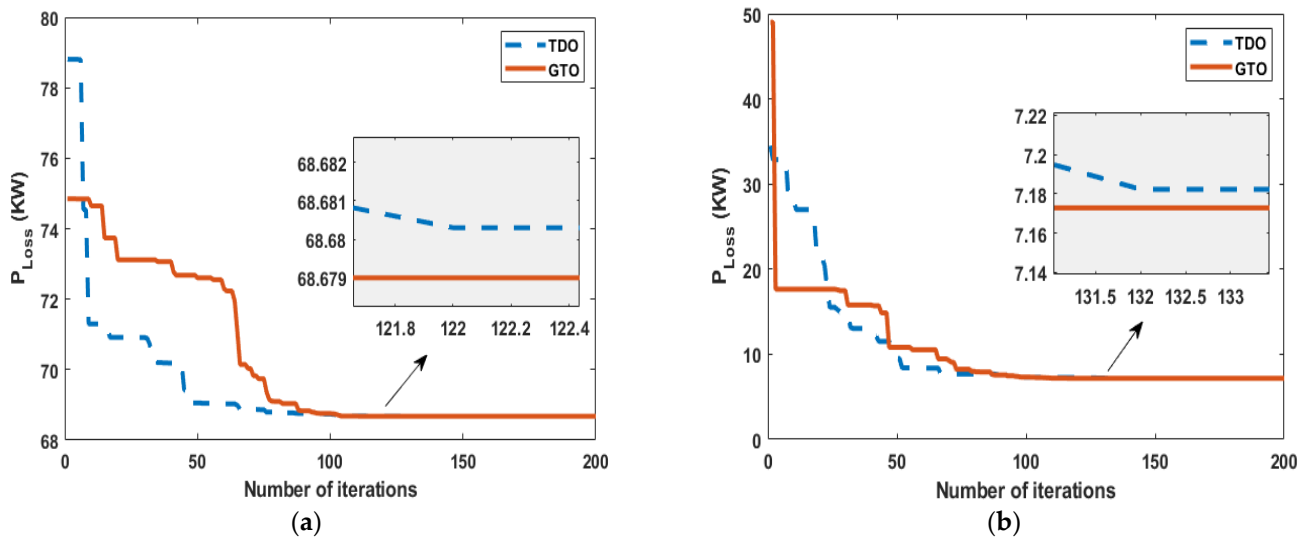


Figure 10. Convergence characteristics of the TDO and GTO algorithms for an IEEE 69-bus system for scenario 1 at different pf: (a) Unity pf (PV type), (b) 0.85 pf (WT type).

4.2.2. Evaluation of Multi-Objective Function (MOF)

In this scenario, the TDO and GTO algorithms are employed to optimize the MOF, using APL, VD, VSI, and OCI to solve the problem of OADG in RDS, considering the CP load model and VP load models for three PV (unity pf) and three WT (0.85 pf).

CP Load Model

Table 15 presents the results of the MOF in terms of APL reduction, VD minimization, VSI maximization, and the minimization of the total operating costs for the optimum placement and sizing of DGs for three PV (unity pf) and three WT (0.85 pf). The total power loss of the system in the base case is (224.60KW + j101.99KVAR); the voltage deviation is 0.09803 p.u., the VSI is 0.6855, and the operating cost is 17.274315 million USD (M\$).

Table 15. Results of OADG for a 69-bus RDN for MOF at unity pf (PV Type) and 0.85 pf (WT type) in a CP load model.

Parameters	Base Case	Unity pf (PV Type)		0.85 pf (WT Type)	
		TDO [P]	GTO [P]	TDO [P]	GTO [P]
APL (KW)	224.60	69.19	69.20	7.21	7.21
APLR (%)	-	69.19%	69.18%	96.79%	96.79%
Location	-	61, 11, 18	11, 61, 17	17, 64, 61	17, 61, 64
DG Size (KW)	-	2000, 682, 441	683, 2000, 444	613, 350, 1678	617, 1691, 338
DG Size (KVAR)	-	-	-	379, 217, 1040	382, 1048, 209
DG Size (KVA)	-	3123	3127	3107	3112
VD (p.u.)	0.09803	0.002093	0.002074	0.000339	0.000332
VSI (p.u.)	0.68548	0.9477	0.9478	0.9773	0.9773
OC (M\$)	17.274315	3.210458	3.193349	5.012274	4.990830
OC _{DG} (M\$)	-	1.913887	1.916338	1.618500	1.621564
DG _M (M\$)	-	7.928960	7.939116	6.705214	6.717909
DG _O (M\$)	-	1.2492	1.2508	1.0564	1.0584
DG _{IC} (M\$)	17.274315	14.302505	14.299603	14.392388	14.388703
OCI	1.0	0.8280	0.8278	0.8332	0.8330

It can be seen from Table 15 that at unity pf (PV type), the APL is reduced to 69.19 KW (69.19%) for the TDO algorithm and 68.20 KW (69.18%) for the GTO algorithm. The VD obtained by employing the TDO and GTO algorithms is 0.002093 p.u. and 0.002074 p.u., respectively, while the value of VSI computed for the TDO and GTO algorithms is 0.9477 p.u.

and 0.9478 p.u., respectively, and the operating cost index for the TDO and GTO algorithms is 8280 and 8278, respectively. Furthermore, the cost savings for the GTO and TDO algorithms at unity pf (PV-type) after 20 years are 17.20% and 17.22%, respectively.

Similarly, at 0.85 pf (WT type), the APL is reduced to 7.21 KW (96.76%) for both the TDO and GTO algorithms. The VD obtained by employing the GTO and TDO algorithms is 0.000339 p.u. and 0.000332 p.u., respectively, while the value of VSI computed for both the TDO and GTO algorithms is 0.9773 p.u., and the operating cost index for the TDO and GTO algorithms is 8332 and 8330, respectively. Moreover, the cost savings for the TDO and GTO algorithms at 0.85 pf (WT type) after 20 years are 16.68% and 16.78%, respectively. It can be concluded that compared to 0.85 pf (WT type), the results of the cost-saving process for unity pf (PV type) are high.

VP Load Model

The results of MOF in terms of APL reduction, VD minimization, VSI maximization, and the minimization of total operating cost for the optimum placement and sizing of DGs for VP load models for three PV (unity pf) and three WT (0.85 pf) are shown in Tables 16 and 17.

It can be seen from Table 16 that at unity pf (PV type), by employing the TDO algorithm, the APL was reduced to 29.44 KW (82.86%) for the industrial load model, for the residential load model, APL is reduced to 38.23 KW (76.87%), and for the commercial load model, APL is reduced to 41.70 KW (73.50%) while by employing the GTO algorithm, the APL is reduced to 29.44 KW (82.86%) for the industrial load model, 38.21 KW (76.88%) for the residential load model; for the commercial load model, APL is reduced to 41.73 KW (73.49%). The obtained VD from the TDO algorithm for an industrial load model is 0.000882 p.u., for a residential load model, it is 0.00117 p.u., and for a commercial load model, it is 0.00129 p.u., while the VD obtained from the GTO algorithms is 0.000876 p.u. for the industrial load model, 0.00117 p.u. for the residential load model, and for the commercial load model, it is 0.00127 p.u. The VSI computed by employing the TDO algorithm for the industrial load model is 0.9714 p.u., for residential is 0.9665 p.u. and for commercial load models is 0.9643 p.u. while for the GTO algorithm, it is 0.9714 p.u., 0.9660 p.u., and 0.9647 p.u. for industrial, residential, and commercial load models, respectively. The operating cost index obtained from the TDO and GTO algorithms for industrial load is 0.8311, for residential 0.8353 and 0.8352, and for commercial 0.8387 and 0.8383, respectively.

Besides this, the cost saving after 20 years for the industrial load model will be 16.89% for both the TDO and GTO algorithms; for a residential load it will be 16.47% and 16.48% for the TDO and GTO algorithms, and for a commercial load, it will be 16.13% and 16.17% for the TDO and GTO algorithms, respectively.

Moreover, the results of the OADG for MOF at 0.85 pf (WT type) are shown in Table 17. By employing TDO, the APL is reduced to 3.95 KW (97.70%) for the industrial load model, 3.93 KW (97.62%) for the residential load model, and 3.88 KW (97.54%) for the commercial load model, while by employing the GTO algorithm, the APL is reduced to 3.96 KW (97.69%), 3.93 KW (97.62%), and 3.88 KW (96.54%) for the industrial, residential, and commercial load models, respectively. The obtained VD from the TDO and GTO algorithms for the industrial load model is 0.0000890 p.u., and for the residential load model, it is 0.000888 p.u., while the VD obtained from the TDO and GTO algorithms for a commercial load model is 0.0000887 p.u. and 0.0000882 p.u., respectively. The VSI computed for the industrial, residential, and commercial load models by employing both the TDO and GTO algorithms is 0.9778 p.u., 0.9777 p.u., and 0.9777 p.u., respectively. The operating cost index obtained from the TDO and GTO algorithms after 20 years for industrial load is 0.8317 and 0.8315, for residential load, it is 0.8336, and for commercial load, it is 0.8358, respectively. Besides this, the cost-saving after 20 years for the industrial load will be 16.83% and 16.85% for the TDO and GTO algorithms, for residential load, it will be 16.65% for both the TDO and GTO algorithms, and for commercial load, it will be 16.42% for both the TDO and GTO algorithms, respectively.

Table 16. Results of OADG for 69 bus RDN for MOF at unity pf (PV Type) in VP load model.

Parameters		Unity pf (PV Type)					
		Industrial		Residential		Commercial	
Base case	APL (KW)	171.72		165.31		157.39	
	VD (p.u.)	0.079855		0.076462		0.072316	
	VSI (p.u.)	0.7151		0.7218		0.7299	
	OC (M\$)	16.902644		16.300692		15.831996	
Parameters		TDO [P]	GTO [P]	TDO [P]	GTO [P]	TDO [P]	GTO [P]
With 3 DGs	APL (KW)	29.44	29.44	38.23	38.21	41.70	41.73
	APLR (%)	82.86%	83.86%	76.87%	76.88%	73.50%	73.49%
	Location	61, 18, 11	18, 61, 11	18, 61, 11	18, 11, 61	18, 61, 11	18, 61, 11
	DG Size (KW)	1996, 429, 616	431, 1996, 614	419, 1887, 593	418, 601, 1882	411, 581, 1796	409, 1798, 590
	DG Size (KVAR)	-	-	-	-	-	-
	DG Size (KVA)	3041	3041	2899	2901	2788	2797
	VD (p.u.)	0.000882	0.000876	0.00117	0.00117	0.00129	0.00127
	VSI (p.u.)	0.9714	0.9714	0.9665	0.9660	0.9643	0.9647
	OC _{DG} (M\$)	3.246820	3.246814	3.319258	3.310582	3.375599	3.337137
	DG _M (M\$)	1.863634	1.863634	1.776612	1.777837	1.708587	1.714102
	DG _O (M\$)	7.720771	7.720771	7.360248	7.365326	7.078431	7.101281
	DG _{IC} (M\$)	1.2164	1.2164	1.1596	1.1604	1.1152	1.1188
	OC _{TDG} (M\$)	14.047625	14.047619	13.615718	13.614146	13.277817	13.271321
	OCI	0.8311	0.8311	0.8353	0.8352	0.8387	0.8383

Table 17. Results of the OADG for a 69-bus RDN for MOF at 0.85 pf (WT type) in the VP load model.

Parameters		0.85 pf (WT Type)					
		Industrial		Residential		Commercial	
Base case	APL (KW)	171.72		165.31		157.39	
	VD (p.u.)	0.079855		0.076462		0.072316	
	VSI (p.u.)	0.7151		0.7218		0.7299	
	OC (M\$)	16.902644		16.300692		15.831996	
Parameters		TDO [P]	GTO [P]	TDO [P]	GTO [P]	TDO [P]	GTO [P]
With 3 DGs	APL (KW)	3.95	3.96	3.93	3.93	3.88	3.88
	APLR (%)	97.70%	97.69%	97.62%	97.62%	97.54%	96.54%
	Location	18, 11, 61	11, 61, 18	18, 61, 11	61, 18, 11	61, 11, 18	61, 18, 11
	DG Size (KW)	422, 612, 1844	622, 1843, 418	406, 1732, 600	1727, 409, 602	1640, 595, 395	1641, 399, 590
	DG Size (KVAR)	220, 327, 775	323, 778, 220	241, 927, 335	928, 236, 352	980, 354, 241	979, 242, 365
	DG Size (KVA)	3167	3171	3123	3130	3066	3071
	VD (p.u.)	0.0000890	0.0000890	0.0000888	0.0000888	0.0000887	0.0000882
	VSI (p.u.)	0.9778	0.9778	0.9777	0.9777	0.9777	0.9777
	OC _{DG} (M\$)	3.8367397	3.8153204	3.862792	3.862786	3.891135	3.891138
	DG _M (M\$)	1.763742	1.766806	1.677945	1.677945	1.611759	1.611759
	DG _O (M\$)	7.306932	7.319626	6.951487	6.951487	6.677286	6.677286
	DG _{IC} (M\$)	1.1512	1.1532	1.0952	1.0952	1.052	1.052
	OC _{TDG} (M\$)	14.058613	14.054953	13.587424	13.587417	13.232180	13.232183
	OCI	0.8317	0.8315	0.8336	0.8336	0.8358	0.8358

It can be concluded that compared to 0.85 pf (WT type), the results of the MOF in terms of APL reduction, the minimization of VD and OCI, and the maximization of VSI are improved at 0.85 pf (WT type). Furthermore, the maximum cost saving is achieved at 0.85 pf (WT-type) for the residential and commercial load models, while for the industrial load model, the maximum cost saving occurs when the DG operates at unity pf (PV type).

5. Conclusions

In this study, two metaheuristic optimization algorithms, the TDO and GTO algorithms, are employed to establish the optimal placement and sizing of renewable-based DGS (PV and WT) at unity and 0.85 pf. The proposed algorithms are utilized to optimize single- and multi-objective functions. A reduction in active and reactive power loss is achieved through optimizing a single-objective function, while a multi-objective function is optimized to reduce the active power loss, minimize the voltage deviation, maximize the voltage stability index, and minimize the total operating cost index. These objectives are achieved by using a multi-objectivity approach, i.e., a weighted sum method. The effectiveness and the validation of the proposed algorithms are examined on IEEE 33-bus and IEEE 69-bus RDNs. As the SOF, the active power loss for both the TDO and GTO algorithms at 0.85 pf is more reduced than other existing optimization algorithms, that is, 93.15% and 96.87% of the initial value for a 33-bus and for a 69-bus RDN, respectively. The proposed algorithms are also examined for PV-DG and WT-DG on IEEE 33- and IEEE 69-bus RDNs, considering voltage-dependent load models such as industrial, residential, and commercial load models; they also show better results compared to the existing optimization techniques, in terms of power loss reduction. For the SOF, the proposed GTO algorithm outperformed the other proposed TDO algorithm in terms of efficiency in converging for a solution, while for MOF, the results of APL minimization for the GTO algorithm are comparable to the other proposed TDO algorithm, but, in terms of other objectives, such as VD minimization, OCI minimization, and VSI maximization, the GTO algorithm offers better results than the TDO algorithm. Therefore, both the GTO and TDO algorithms can be used for the optimal placement and sizing of DGs in DN. In the future, subsequent studies can be extended to the higher bus systems while considering the intermittent nature of renewable sources and the uncertainties related to the load demand, working with daily load patterns and seasonal variations.

Author Contributions: Conceptualization, H.U.R. and A.H.; methodology, H.U.R., W.H., S.A.A.K. and S.A.A.; software, H.U.R., A.H. and S.A.A.; validation, H.U.R., W.H., M.H. and S.A.A.K.; formal analysis, M.H., A.H. and W.H.; investigation, H.U.R. and S.A.A.K.; resources, A.H., M.H. and W.H.; data curation, M.H., A.H., W.H. and S.A.A.; writing—original draft preparation, H.U.R., W.H., M.H. and S.A.A.K.; writing—review and editing, H.U.R., W.H., M.H. and S.A.A.K.; visualization, M.H., A.H. and W.H.; supervision, S.A.A.K. and W.H.; project administration, S.A.A.K. and W.H.; funding acquisition, A.H. and W.H. All authors have read and agreed to the published version of the manuscript.

Funding: This research received no external funding.

Data Availability Statement: Not applicable.

Conflicts of Interest: The authors declare no conflict of interest.

Abbreviations

RDN	Radial Distribution Network	OCI	Operating Cost Index
VD	Voltage Deviation	P_{DG}	Active Power of DG
APL	Active Power Loss	PWF	Present Worth Factor
QPL	Reactive Power Loss	DG_M	DG maintenance cost
VSI	Voltage Stability Index	DG_O	DG operational cost
DG	Distributed Generations	DG_{INV}	DG investment cost
OADG	Optimal Allocation of DG	OC_{TDG}	Total operating cost of DG
GTO	Artificial Gorilla Troops Optimization	Inf_R	Inflation Rate
TDO	Tasmanian Devil Optimization	Int_R	Interest Rate

Appendix A

The flow chart in Figure 1 for the optimal allocation of the DG with the GTO algorithm is explained through pseudo code for greater clarity in Algorithm A1.

Algorithm A1: Pseudo Code of GTO algorithm

```

1.      Set size of population (gorilla's)  $N$ , maximum iteration  $T$ , upper bound  $ub$ , lower bound  $lb$ 
      GTO parameters  $p$  and  $\beta$ 
2.      Initialize the random gorilla locations  $X_i$  ( $i = 1, 2, 3, \dots, N$ )
3.      Calculate the objective fitness function for each gorilla
4.      while (Termination criteria not met) do
5.          Update the value of  $C$  using Equation (29)
6.          Update the value of  $L$  using Equation (31)
7.          % Exploration phase
8.          for  $i = 1: N$  do
9.              if  $rand < p$  then
10.                 Gorilla location is updated using Equation (28a)
11.             else
12.                 if  $rand \geq 0.5$  then
13.                     Gorilla location is updated using Equation (28b)
14.                 else
15.                     Gorilla location is updated using Equation (28c)
16.                 end if
17.             end if
18.         end for
19.         Calculate the objective fitness function for updated gorilla location
20.         If the fitness value of newly gorilla is better than the previous gorilla, replace with previous.
21.         Set the gorilla location best location so far
22.         % Exploitation phase
23.         for  $i = 1: N$  do
24.             if  $C \geq W$  then
25.                 Gorilla location is updated using Equation (34)
26.             else
27.                 Gorilla location is updated using Equation (37)
28.             end if
29.         end for
30.         Calculate the objective fitness function for updated gorilla location
31.         If the fitness value of newly gorilla is better than the previous gorilla, replace with previous.
32.         Set the gorilla location best location so far
33.     end while
34.     Display the best solution

```

Similarly, the flow chart in Figure 2 for the optimal allocation of the DG via the GTO algorithm is explained through pseudo code for greater clarity in Algorithm A2.

Algorithm A2: Pseudo Code of TDO algorithm

```

1. Set the size of population (Tasmanian devils) N, maximum iteration T, upper bound ub, lower bound lb
2. Initialize the random Tasmanian devil locations
3. Calculate the objective fitness function for each Tasmanian devil
4. while (Termination criteria not met) do
8.   for  $i = 1: N$  do
       pr = rand
9.   if pr < 0.5 then
       % Exploration phase (Selection of carrion and feeding by eating them)
11.    Choose the carrion by using Equation (41)
19.    Calculate the objective fitness function for the selected carrion then
20.    New location of the Tasmanian devil is calculated by using Equation (42) then
       Location of the Tasmanian devil is updated using Equation (43) based on the
       objective function fitness value
       else
21.    % Exploitation phase (Selection of prey and attacking)
22.    Choose the prey by using Equation (44)
23.    Calculate the objective fitness function for the selected prey then
24.    New location of the Tasmanian devil is calculated by using Equation (45) then
25.    Location of the Tasmanian devil is updated using Equation (46) based on the
       objective function fitness value
       Chasing of prey
       The value of neighborhood radius (r) for chasing process is calculated by using Equation (47)
       New location of the Tasmanian devil is for chasing process is calculated by using Equation (48)
       Location of the Tasmanian devil is updated using Equation (49) based on the
       objective function fitness value
28.   end if
29.   Calculate the objective fitness function for updated Tasmanian devil location
30.   If the fitness value of new Tasmanian devil is better than the previous, replace with previous.
       Keep the best solution so far.
31.   end for
       end while
32.   Display the best solution

```

The results of Table A1 at unity pf show that with the integration of the three DGs, reactive power loss (QPL) is reduced to 49.22 KVAR for both the TDO and GTO algorithms, which is a 65.44% reduction with respect to the base value. Similarly, from Table A2, it can be seen that at 0.85 pf, the QPL is reduced to 11.68 KVAR for both the GTO and TDO algorithms after the integration of three DGs, which is a 91.80% reduction with respect to the base value. It can be concluded that the maximum reduction of the QPL is at 0.85 pf (WT type).

Table A1. Results of OADG for a 33-bus RDN for SOF (QPL minimization) at unity pf (PV type) in a CP load model.

Methods	Location	DG Size (KVAR)	QPL (KVAR) QPLR (%)	VD (p.u.)	VSI (p.u.)
Base case	-	-	142.44	0.1328	0.6672
TDO [P]	13, 24, 30	926, 1135, 1160	49.22 (65.44)	0.011766	0.8901
GTO [P]	24, 30, 13	1135, 1160, 926	49.22 (65.44)	0.011766	0.8901

Table A2. Results of OADG for a 33-bus RDN for SOF (QPL minimization) at 0.85 pf (WT type) in a CP load model.

Methods	Location	DG Size		QPL (KVAR) QPLR (%)	VD (p.u.)	VSI (p.u.)
		(KW)	(KVAR)			
Base case	-	-	-	142.44	0.1328	0.6672
TDO [P]	24, 13, 30	1104, 867, 1298	599, 494, 804	11.68 (91.80%)	0.000631	0.9671
GTO [P]	24, 13, 30	1102, 869, 1299	599, 492, 805	11.68 (91.80%)	0.000631	0.9671

The QPL in the base case for an industrial load model is 110.42 KVAR, for a residential load model, it is 107.19 KVAR, and for a commercial load model, it is 102.70 KVAR. The results of the SOF, based on QPL minimization for the optimum placement and sizing of multiple DGs at unity pf (PV-type), are presented in Table A3. It can be seen that after the integration of three DGs, the QPL is reduced to 24.54 KVAR (77.77%) for the industrial load model, for residential APL, it is reduced to 29.48 KVAR (72.49%), and for a commercial load model, it is reduced to 31.24 KVAR (65.68%) for both the TDO and GTO algorithms.

Table A3. Results of OADG for a 33-bus RDN for SOP (QPL minimization) at unity pf (PV type) in a VP load model.

Parameters		Unity pf (PV Type)		
		Industrial	Residential	Commercial
Base case	QPL (KVAR)	110.42	107.19	102.70
	VD (p.u.)	0.098637	0.097821	0.094018
	VSI (p.u.)	0.70741	0.70953	0.71526
TDO [P]	QPL (KVAR)	24.54	29.48	31.24
	QPLR (%)	77.77	72.49	65.68
	Location	13, 30, 24	30, 24, 13	13, 24, 30
	DG Size (KW)	901, 1112, 1130	1059, 1105, 849	808, 1085, 1016
	DG Size (KVAR)	-	-	-
	DG Size (KVA)	3143	3013	2909
	VD (p.u.)	0.005964	0.007305	0.007765
	VSI (p.u.)	0.9208	0.9127	0.9103
GTO [P]	QPL (KVAR)	24.54	29.48	31.24
	QPLR (%)	77.77	72.49	65.68
	Location	13, 30, 24	24, 30, 13	13, 30, 24
	DG Size (KW)	901, 1112, 1130	1105, 1059, 849	808, 1016, 1085
	DG Size (KVAR)	-	-	-
	DG Size (KVA)	3143	3013	2909
	VD (p.u.)	0.005964	0.007305	0.007765
	VSI (p.u.)	0.9208	0.9127	0.9103

Similarly, the results of OADG for QPL reduction at 0.85 pf (WT type) for the different load models are described in Table A4. The QPL for the industrial load model is reduced to 8.66 KVAR (92.15%), for the residential load model, QPL is reduced to 8.50 KVAR (92.07%), and for the commercial load model, QPL is reduced to 8.41 KVAR (91.81%) for both the TDO and GTO algorithms. From the results of Tables A3 and A4, it can be concluded that with the integration of three DGs, the QPL minimization at 0.85pf (WT type) is at maximum compared to unity pf.

The results of OADG at unity pf (PV type) for QPL minimization in a CP load model are presented in Table A5. It can be seen from the table that with the integration of the DGs, QPL is reduced to 31.63 KVAR for both the TDO and GTO algorithms, which is a 68.99% reduction with respect to the base value.

Similarly, the QPL is reduced to 3.96 KVAR for both the GTO and TDO algorithms after the integration of DGs, which is a 96.12% reduction with respect to the base value, as

can be seen from Table A6. From the results, it can be concluded that the QPL minimization is at maximum at 0.85 pf (WT type), compared to the unity pf (PV type).

Table A4. Results of OADG for a 33-bus RDN for SOF (QPL minimization) at 0.85 pf (WT type) in a VP load model.

Parameters		0.85 pf (WT Type)		
		Industrial	Residential	Commercial
Base case	QPL (KVAR)	110.42	107.19	102.70
	VD (p.u.)	0.098637	0.097821	0.094018
	VSI (p.u.)	0.70741	0.70953	0.71526
TDO [P]	QPL (KVAR)	8.66	8.50	8.41
	QPLR (%)	92.15	92.07	91.81
	Location	24, 13, 30	24, 30, 13	13, 24, 30
	DG Size (KW)	1128, 895, 1097	1092, 1105, 825	777, 1065, 1092
	DG Size (KVAR)	457, 259, 680	505, 685, 329	356, 523, 677
	DG Size (KVA)	3418	3382	3221
	VD (p.u.)	0.000542	0.000533	0.000518
	VSI (p.u.)	0.9694	0.9699	0.9705
GTO [P]	QPL (KVAR)	8.66	8.50	8.41
	QPLR (%)	92.15	92.07	91.81
	Location	30, 13, 24	24, 13, 30	30, 24, 13
	DG Size (KW)	1097, 895, 1128	1091, 1106, 825	1092, 1065, 777
	DG Size (KVAR)	680, 259, 457	504, 685, 329	677, 522, 356
	DG Size (KVA)	3418	3382	3321
	VD (p.u.)	0.000541	0.000535	0.000517
	VSI (p.u.)	0.9695	0.9699	0.9705

Table A5. Results of OADG for a 69-bus RDN for QPL minimization at unity pf (PV Type) in a CP load model.

Methods	Location	DG Size (KVAR)	QPL (KVAR) QPLR (%)	VD (p.u.)	VSI (p.u.)
Base case	-	-	101.99	0.09803	0.68548
TDO [P]	50, 17, 61	800, 617, 2000	31.63 (68.99%)	0.003804	0.9371
GTO [P]	17, 61, 50	617, 2000, 800	31.63 (68.99%)	0.003804	0.9371

Table A6. Results of OADG for a 69-bus RDN for QPL minimization at 0.85 pf (WT type) with a CP load model.

Methods	Location	DG Size		QPL (KVAR) QPLR (%)	VD (p.u.)	VSI (p.u.)
		(KW)	(KVAR)			
Base case	-	-	-	101.99	0.09803	0.68548
TDO [P]	50, 12, 61	830, 1076 1700	503, 667 1054	3.96 (96.12%)	0.00176	0.9577
GTO [P]	50, 12, 61	830, 1076 1700	503, 667 1054	3.96 (96.12%)	0.00176	0.9577

Furthermore, the QPL in the base case for the industrial load model is 79.23 KVAR, for the residential load model is 76.52 KVAR, and for the commercial load model, it is 73.13 KVAR. The results of the SOF based on QPL minimization for the optimum placement and sizing of multiple DGs at unity pf (PV-type) are presented in Table A7. After the integration of DGs, the QPL is reduced to 14.45 KVAR (81.76%) for the industrial load model, 18.23 KVAR (76.17%) for the residential load model, and QPL is reduced to 19.73 KVAR (73.02%) for the commercial load model for both the TDO and GTO algorithms.

Table A7. Results of OADG for a 69-bus RDN for QPL minimization at unity pf (PV type) in a VP load model.

Parameters		Unity pf (PV Type)		
		Industrial	Residential	Commercial
Base case	QPL (KVAR)	79.23	76.52	73.13
	VD (p.u.)	0.079855	0.076462	0.072316
	VSI (p.u.)	0.71505	0.7218	0.72986
TDO [P]	QPL (KVAR)	14.45	18.23	19.73
	QPLR (%)	81.76	76.17	73.02
	Location	61, 50, 17	50, 17, 61	17, 50, 61
	DG Size (KW)	1943, 798, 611	796, 594, 1833	581, 793, 1748
	DG Size (KVAR)	-	-	-
	DG Size (KVA)	3352	3223	3122
	VD (p.u.)	0.002071	0.002477	0.002617
	VSI (p.u.)	0.9559	0.9512	0.9498
GTO [P]	QPL (KVAR)	14.45	18.23	19.73
	QPLR (%)	81.76	76.17	73.02
	Location	61, 50, 17	17, 50, 61	50, 61, 17
	DG Size (KW)	1942, 799, 612	594, 796, 1833	793, 1748, 581
	DG Size (KVAR)	-	-	-
	DG Size (KVA)	3553	3223	3122
	VD (p.u.)	0.002068	0.002477	0.002618
	VSI (p.u.)	0.9558	0.9512	0.9498

Similarly, the results of OADG for QPL reduction at 0.85 pf (WT type) for different load models are described in Table A8. The QPL for the industrial load model is reduced to 2.24 KVAR (97.17%), for the residential model, it is reduced to 2.17 KVAR (97.16%), and for the commercial load model, QPL is reduced to 2.12 KVAR (97.11%) for both the TDO and GTO algorithms.

Table A8. Results of OADG for a 69-bus RDN for SOF (QPL minimization) at 0.85 pf (WT type) in a VP load model.

Parameters		Unity pf (PV Type)		
		Industrial	Residential	Commercial
Base case	QPL (KVAR)	79.23	76.52	73.13
	VD (p.u.)	0.079855	0.076462	0.072316
	VSI (p.u.)	0.71505	0.7218	0.72986
TDO [P]	QPL (KVAR)	2.24	2.17	2.12
	QPLR (%)	97.17	97.16	97.11
	Location	18, 50, 61	17, 50, 61	50, 61, 17
	DG Size (KW)	627, 836, 1837	602, 824, 1755	828, 1709, 582
	DG Size (KVAR)	347, 517, 790	362, 511, 959	513, 1034, 360
	DG Size (KVA)	3691	3670	3656
	VD (p.u.)	0.000353	0.000283	0.000230
	VSI (p.u.)	0.9808	0.9811	0.9818
GTO [P]	QPL (KVAR)	2.24	2.17	2.12
	QPLR (%)	97.17	97.16	97.11
	Location	18, 50, 61	17, 50, 61	50, 61, 17
	DG Size (KW)	627, 836, 1837	602, 824, 1755	828, 1709, 582
	DG Size (KVAR)	347, 517, 790	362, 511, 959	513, 1034, 360
	DG Size (KVA)	3691	3670	3656
	VD (p.u.)	0.000353	0.000283	0.000230
	VSI (p.u.)	0.9808	0.9811	0.9818

References

1. Karunarathne, E.; Pasupuleti, J.; Ekanayake, J.; Almeida, D. Optimal Placement and Sizing of DGs in Distribution Networks Using MLPSO Algorithm. *Energies* **2020**, *13*, 6185. [\[CrossRef\]](#)
2. Sharma, S.; Bhattacharjee, S.; Bhattacharya, A. Quasi-Oppositional Swine Influenza Model Based Optimization with Quarantine for optimal allocation of DG in radial distribution network. *Int. J. Electr. Power Energy Syst.* **2016**, *74*, 348–373. [\[CrossRef\]](#)
3. Haider, W.; Hassan, S.; Mehdi, A.; Hussain, A.; Adjayeng, G.; Kim, C.-H. Voltage Profile Enhancement and Loss Minimization Using Optimal Placement and Sizing of Distributed Generation in Reconfigured Network. *Machines* **2021**, *9*, 20. [\[CrossRef\]](#)
4. Paliwal, P.; Patidar, N.; Nema, R. Planning of grid integrated distributed generators: A review of technology, objectives and techniques. *Renew. Sustain. Energy Rev.* **2014**, *40*, 557–570. [\[CrossRef\]](#)
5. Mahmoud, K.; Yorino, N.; Ahmed, A. Optimal Distributed Generation Allocation in Distribution Systems for Loss Minimization. *IEEE Trans. Power Syst.* **2015**, *31*, 960–969. [\[CrossRef\]](#)
6. Xiong, X.; Wu, W.; Li, N.; Yang, L.; Zhang, J.; Wei, Z. Risk-Based Multi-Objective Optimization of Distributed Generation Based on GPSO-BFA Algorithm. *IEEE Access* **2019**, *7*, 30563–30572. [\[CrossRef\]](#)
7. Sa'Ed, J.A.; Amer, M.; Bodair, A.; Baransi, A.; Favuzza, S.; Zizzo, G. A Simplified Analytical Approach for Optimal Planning of Distributed Generation in Electrical Distribution Networks. *Appl. Sci.* **2019**, *9*, 5446. [\[CrossRef\]](#)
8. Kashyap, M.; Kansal, S.; Verma, R. Sizing and Allocation of DGs in A Passive Distribution Network Under Various Loading Scenarios. *Electr. Power Syst. Res.* **2022**, *209*, 108046. [\[CrossRef\]](#)
9. Adewuyi, O.B.; Adeagbo, A.P.; Adebayo, I.G.; Howlader, H.O.R.; Sun, Y. Modified Analytical Approach for PV-DGs Integration into a Radial Distribution Network Considering Loss Sensitivity and Voltage Stability. *Energies* **2021**, *14*, 7775. [\[CrossRef\]](#)
10. Montoya, O.D.; Gil-González, W.; Grisales-Noreña, L. An exact MINLP model for optimal location and sizing of DGs in distribution networks: A general algebraic modeling system approach. *Ain Shams Eng. J.* **2019**, *11*, 409–418. [\[CrossRef\]](#)
11. Garfi, O.; Aloui, H. Multiple distributed generations placement and sizing based on voltage stability index and power loss minimization. *Turk. J. Electr. Eng. Comput. Sci.* **2019**, *27*, 4567–4579. [\[CrossRef\]](#)
12. Essallah, S.; Khedher, A.; Bouallegue, A. Integration of distributed generation in electrical grid: Optimal placement and sizing under different load conditions. *Comput. Electr. Eng.* **2019**, *79*, 106461. [\[CrossRef\]](#)
13. Vita, V. Development of a Decision-Making Algorithm for the Optimum Size and Placement of Distributed Generation Units in Distribution Networks. *Energies* **2017**, *10*, 1433. [\[CrossRef\]](#)
14. Bayat, A.; Bagheri, A. Optimal active and reactive power allocation in distribution networks using a novel heuristic approach. *Appl. Energy* **2018**, *233–234*, 71–85. [\[CrossRef\]](#)
15. Nguyen, T.P.; Tran, T.T.; Vo, D.N. Improved stochastic fractal search algorithm with chaos for optimal determination of location, size, and quantity of distributed generators in distribution systems. *Neural Comput. Appl.* **2018**, *31*, 7707–7732. [\[CrossRef\]](#)
16. Karunarathne, E.; Pasupuleti, J.; Ekanayake, J.; Almeida, D. Network loss reduction and voltage improvement by optimal placement and sizing of distributed generators with active and reactive power injection using fine-tuned PSO. *Indones. J. Electr. Eng. Comput. Sci.* **2021**, *21*, 647–656. [\[CrossRef\]](#)
17. Shahzad, M.; Akram, W.; Arif, M.; Khan, U.; Ullah, B. Optimal Siting and Sizing of Distributed Generators by Strawberry Plant Propagation Algorithm. *Energies* **2021**, *14*, 1744. [\[CrossRef\]](#)
18. Samal, P.; Panigrahy, D. A Novel Technique Based on Aquila Optimiser Algorithm for Optimal Integration of Distributed Generations in the Distribution System. *Process. Integr. Optim. Sustain.* **2022**, 0123456789. [\[CrossRef\]](#)
19. Hassan, A.S.; Sun, Y.; Wang, Z. Multi-objective for optimal placement and sizing DG units in reducing loss of power and enhancing voltage profile using BPSO-SLFA. *Energy Rep.* **2020**, *6*, 1581–1589. [\[CrossRef\]](#)
20. Malika, B.K.; Pattanaik, V.; Sahu, B.K.; Rout, P.K. *Quasi-Oppositional Forensic-Based Investigation for Optimal DG Selection for Power Loss Minimization*; no. 0123456789; Springer Nature: Singapore, 2022. [\[CrossRef\]](#)
21. Tiwari, V.; Dubey, H.M.; Pandit, M. Assessment of Optimal Size and Location of DG/CB in Distribution Systems using Coulomb-Franklin's Algorithm. *J. Inst. Eng. Ser. B* **2022**, *103*, 1885–1908. [\[CrossRef\]](#)
22. Moaidi, F.; Moaidi, M. Optimal Placement and Sizing of Distributed Generation in Microgrid for Power Loss Reduction and Voltage Profile Improvement. *World Acad. Sci. Eng. Technol. Int. J. Energy Power Eng.* **2019**, *13*, 26–31.
23. Truong, K.H.; Nallagownden, P.; Elamvazuthi, I.; Vo, D.N. A Quasi-Oppositional-Chaotic Symbiotic Organisms Search algorithm for optimal allocation of DG in radial distribution networks. *Appl. Soft Comput.* **2020**, *88*, 106067. [\[CrossRef\]](#)
24. Mahfoud, R.J.; Sun, Y.; Alkayem, N.F.; Alhelou, H.H.; Siano, P.; Shafie-Khah, M. A Novel Combined Evolutionary Algorithm for Optimal Planning of Distributed Generators in Radial Distribution Systems. *Appl. Sci.* **2019**, *9*, 3394. [\[CrossRef\]](#)
25. Hemeida, M.; Alkhalaf, S.; Mohamed, A.-A.; Ibrahim, A.; Senjyu, T. Distributed Generators Optimization Based on Multi-Objective Functions Using Manta Rays Foraging Optimization Algorithm (MRFO). *Energies* **2020**, *13*, 3847. [\[CrossRef\]](#)
26. Akbar, M.I.; Kazmi, S.A.A.; Alrumayh, O.; Khan, Z.A.; Altamimi, A.; Malik, M.M. A Novel Hybrid Optimization-Based Algorithm for the Single and Multi-Objective Achievement With Optimal DG Allocations in Distribution Networks. *IEEE Access* **2022**, *10*, 25669–25687. [\[CrossRef\]](#)
27. Ali, A.; Keerio, M.U.; Laghari, J.A. Optimal Site and Size of Distributed Generation Allocation in Radial Distribution Network Using Multi-objective Optimization. *J. Mod. Power Syst. Clean Energy* **2021**, *9*, 404–415. [\[CrossRef\]](#)
28. Selim, A.; Kamel, S.; Jurado, F. Efficient optimization technique for multiple DG allocation in distribution networks. *Appl. Soft Comput.* **2019**, *86*, 105938. [\[CrossRef\]](#)

29. Selim, A.; Kamel, S.; Alghamdi, A.S.; Jurado, F. Optimal Placement of DGs in Distribution System Using an Improved Harris Hawks Optimizer Based on Single- and Multi-Objective Approaches. *IEEE Access* **2020**, *8*, 52815–52829. [[CrossRef](#)]
30. Eid, A.; Kamel, S.; Korashy, A.; Khurshaid, T. An Enhanced Artificial Ecosystem-Based Optimization for Optimal Allocation of Multiple Distributed Generations. *IEEE Access* **2020**, *8*, 178493–178513. [[CrossRef](#)]
31. Sambaiah, K.S.; Jayabarathi, T. Optimal Allocation of Renewable Distributed Generation and Capacitor Banks in Distribution Systems using Salp Swarm Algorithm. *Int. J. Renew. Energy Res.* **2019**, *9*, 96–107. [[CrossRef](#)]
32. Rajalakshmi, J.; Durairaj, S. Application of multi-objective optimization algorithm for siting and sizing of distributed generations in distribution networks. *J. Comb. Optim.* **2020**, *41*, 267–289. [[CrossRef](#)]
33. Anbuchandran, S.; Rengaraj, R.; Bhuvanesh, A.; Karuppasampandiyar, M. A Multi-objective Optimum Distributed Generation Placement Using Firefly Algorithm. *J. Electr. Eng. Technol.* **2021**, *17*, 945–953. [[CrossRef](#)]
34. Murty, V.V.S.N.; Kumar, A. Optimal DG integration and network reconfiguration in microgrid system with realistic time varying load model using hybrid optimisation. *IET Smart Grid* **2019**, *2*, 192–202. [[CrossRef](#)]
35. Kumar, S.; Mandal, K.K.; Chakraborty, N. Optimal DG placement by multi-objective opposition based chaotic differential evolution for techno-economic analysis. *Appl. Soft Comput.* **2019**, *78*, 70–83. [[CrossRef](#)]
36. Al-Ammar, E.A.; Farzana, K.; Waqar, A.; Aamir, M.; Saifullah; Haq, A.U.; Zahid, M.; Batool, M. ABC algorithm based optimal sizing and placement of DGs in distribution networks considering multiple objectives. *Ain Shams Eng. J.* **2020**, *12*, 697–708. [[CrossRef](#)]
37. Kumar, S.; Mandal, K.; Chakraborty, N. A novel opposition-based tuned-chaotic differential evolution technique for techno-economic analysis by optimal placement of distributed generation. *Eng. Optim.* **2019**, *52*, 303–324. [[CrossRef](#)]
38. Devi, S.A.C.; Yamuna, K.; Sornalatha, M. Multi-objective optimization of optimal placement and sizing of multiple DG placements in radial distribution system using stud krill herd algorithm. *Neural Comput. Appl.* **2021**, *33*, 13619–13634. [[CrossRef](#)]
39. Godha, N.R.; Bapat, V.N.; Korachagaon, I. Ant colony optimization technique for integrating renewable DG in distribution system with techno-economic objectives. *Evol. Syst.* **2022**, *13*, 485–498. [[CrossRef](#)]
40. Abid, S.; Apon, H.J.; Morshed, K.A.; Ahmed, A. Optimal Planning of Multiple Renewable Energy-Integrated Distribution System With Uncertainties Using Artificial Hummingbird Algorithm. *IEEE Access* **2022**, *10*, 40716–40730. [[CrossRef](#)]
41. Onlam, A.; Yodphet, D.; Chatthaworn, R.; Surawanitkun, C.; Siritaratiwat, A.; Khunkitti, P. Power Loss Minimization and Voltage Stability Improvement in Electrical Distribution System via Network Reconfiguration and Distributed Generation Placement Using Novel Adaptive Shuffled Frogs Leaping Algorithm. *Energies* **2019**, *12*, 553. [[CrossRef](#)]
42. Duong, M.; Pham, T.; Nguyen, T.; Doan, A.; Tran, H. Determination of Optimal Location and Sizing of Solar Photovoltaic Distribution Generation Units in Radial Distribution Systems. *Energies* **2019**, *12*, 174. [[CrossRef](#)]
43. Nowdeh, S.A.; Davoudkhani, I.F.; Moghaddam, M.H.; Najmi, E.S.; Abdelaziz, A.Y.; Ahmadi, A.; Razavi, S.; Gandoman, F.H. Fuzzy multi-objective placement of renewable energy sources in distribution system with objective of loss reduction and reliability improvement using a novel hybrid method. *Appl. Soft Comput.* **2019**, *77*, 761–779. [[CrossRef](#)]
44. Kamel, S.; Awad, A.; Abdel-Mawgoud, H.; Jurado, F. Optimal DG allocation for enhancing voltage stability and minimizing power loss using hybrid gray wolf optimizer. *Turk. J. Electr. Eng. Comput. Sci.* **2019**, *27*, 2947–2961. [[CrossRef](#)]
45. Nagaballi, S.; Kale, V.S. Pareto optimality and game theory approach for optimal deployment of DG in radial distribution system to improve techno-economic benefits. *Appl. Soft Comput.* **2020**, *92*, 106234. [[CrossRef](#)]
46. Eid, A. Allocation of distributed generations in radial distribution systems using adaptive PSO and modified GSA multi-objective optimizations. *Alex. Eng. J.* **2020**, *59*, 4771–4786. [[CrossRef](#)]
47. Kamel, S.; Selim, A.; Ahmed, W.; Jurado, F. Single- and multi-objective optimization for photovoltaic distributed generators implementation in probabilistic power flow algorithm. *Electr. Eng.* **2019**, *102*, 331–347. [[CrossRef](#)]
48. Deb, G.; Chakraborty, K.; Deb, S. Modified Spider Monkey Optimization-Based Optimal Placement of Distributed Generators in Radial Distribution System for Voltage Security Improvement. *Electr. Power Compon. Syst.* **2020**, *48*, 1006–1020. [[CrossRef](#)]
49. Waqar, A.; Subramaniam, U.; Farzana, K.; Elavarasan, R.M.; Habib, H.U.R.; Zahid, M.; Hossain, E. Analysis of Optimal Deployment of Several DGs in Distribution Networks Using Plant Propagation Algorithm. *IEEE Access* **2020**, *8*, 175546–175562. [[CrossRef](#)]
50. Yuvaraj, T.; Devabalaji, K.; Prabakaran, N.; Alhelou, H.H.; Manju, A.; Pal, P.; Siano, P. Optimal Integration of Capacitor and Distributed Generation in Distribution System Considering Load Variation Using Bat Optimization Algorithm. *Energies* **2021**, *14*, 3548. [[CrossRef](#)]
51. Sellami, R.; Sher, F.; Neji, R. An improved MOPSO algorithm for optimal sizing & placement of distributed generation: A case study of the Tunisian offshore distribution network (ASHTART). *Energy Rep.* **2022**, *8*, 6960–6975. [[CrossRef](#)]
52. Ramshanker, A.; Isaac, J.R.; Jeyaraj, B.E.; Swaminathan, J.; Kuppan, R. Optimal DG Placement in Power Systems Using a Modified Flower Pollination Algorithm. *Energies* **2022**, *15*, 8516. [[CrossRef](#)]
53. Gümüş, T.E.; Emiroglu, S.; Yalcin, M.A. Optimal DG allocation and sizing in distribution systems with Thevenin based impedance stability index. *Int. J. Electr. Power Energy Syst.* **2023**, *144*, 108555. [[CrossRef](#)]
54. Subbaramaiah, K.; Sujatha, P. Optimal DG unit placement in distribution networks by multi-objective whale optimization algorithm & its techno-economic analysis. *Electr. Power Syst. Res.* **2023**, *214*, 108869. [[CrossRef](#)]
55. Alizadeh, S.; Mahdavian, M.; Ganji, E. Optimal placement and sizing of photovoltaic power plants in power grid considering multi-objective optimization using evolutionary algorithms. *J. Electr. Syst. Inf. Technol.* **2023**, *10*, 7. [[CrossRef](#)]

56. Ehsan, A.; Yang, Q. Optimal integration and planning of renewable distributed generation in the power distribution networks: A review of analytical techniques. *Appl. Energy* **2018**, *210*, 44–59. [[CrossRef](#)]
57. Nguyen, T.P.; Nguyen, T.A.; Phan, T.V.H.; Vo, D.N. A comprehensive analysis for multi-objective distributed generations and capacitor banks placement in radial distribution networks using hybrid neural network algorithm. *Knowl.-Based Syst.* **2021**, *231*, 107387. [[CrossRef](#)]
58. Raut, U.; Mishra, S. An improved Elitist–Jaya algorithm for simultaneous network reconfiguration and DG allocation in power distribution systems. *Renew. Energy Focus* **2019**, *30*, 92–106. [[CrossRef](#)]
59. Abdollahzadeh, B.; Gharehchopogh, F.S.; Mirjalili, S. Artificial gorilla troops optimizer: A new nature-inspired metaheuristic algorithm for global optimization problems. *Int. J. Intell. Syst.* **2021**, *36*, 5887–5958. [[CrossRef](#)]
60. Dehghani, M.; Hubalovsky, S.; Trojovský, P. Tasmanian Devil Optimization: A New Bio-Inspired Optimization Algorithm for Solving Optimization Algorithm. *IEEE Access* **2022**, *10*, 19599–19620. [[CrossRef](#)]
61. Baran, M.E.; Wu, F.F. Network reconfiguration in distribution systems for loss reduction and load balancing. *IEEE Trans. Power Deliv.* **1989**, *4*, 1401–1407. [[CrossRef](#)]
62. Baran, M.; Wu, F.F. Optimal sizing of capacitors placed on a radial distribution system. *IEEE Trans. Power Deliv.* **1989**, *4*, 735–743. [[CrossRef](#)]

Disclaimer/Publisher’s Note: The statements, opinions and data contained in all publications are solely those of the individual author(s) and contributor(s) and not of MDPI and/or the editor(s). MDPI and/or the editor(s) disclaim responsibility for any injury to people or property resulting from any ideas, methods, instructions or products referred to in the content.